5-2-2018

Toward a Diffusive, Non-Destructive Approach to Measuring Stable Isotopes of Water within Tree Stems

Scott A. Raulerson
Georgia State University

TOWARD A DIFFUSIVE, NON-DESTRUCTIVE APPROACH TO MEASURING STABLE ISOTOPES OF WATER WITHIN TREE STEMS

by

SCOTT RAULERSON

Under the Direction of Luke A. Pangle, Ph.D.

ABSTRACT

Traditional methodologies for measuring ratios of stable isotopes within the xylem water of trees involves destructive coring of the stem. A recent approach involves permanently installed probes within the stem, and an on-site assembly of pumps, switching valves, gas lines, and climate-controlled structure for field deployment of a laser spectrometer. The former method limits the possible temporal resolution of sampling, and sample size, while the latter may not be feasible for many research groups. Researchers have used direct liquid-vapor equilibration as a method to measure isotope ratios of the water in soil pores. Typically, this is done by placing soil samples in a fixed container, and allowing the liquid water within the soil to come into isotopic equilibrium with the headspace of the container. We present a novel approach to measuring xylem water that relies on liquid-vapor equilibration, built from the principals applied to soil samples.

INDEX WORDS: Xylem water, Stable isotopes, Diffusive sampling, Transpiration, Laser Spectroscopy, Ecohydrology

TOWARD A DIFFUSIVE, NON-DESTRUCTIVE APPROACH TO MEASURING STABLE ISOTOPES OF WATER WITHIN TREE STEMS

by

SCOTT RAULERSON

A Thesis Submitted in Partial Fulfillment of the Requirements for the Degree of

Master of Science

in the College of Arts and Sciences

Georgia State University

2018

TOWARD A DIFFUSIVE, NON-DESTRUCTIVE APPROACH TO MEASURING STABLE ISOTOPES OF WATER WITHIN TREE STEMS

by

SCOTT RAULERSON

Committee Chair: Luke Pangle

Committee: Luke Pangle

Brian Meyer

Rebekah Chapman

Electronic Version Approved:

Office of Graduate Studies

College of Arts and Sciences

Georgia State University

May 2018

DEDICATION

I would like to thank Don & Pat Raulerson for their support in my education. A special thanks to Maia Hart, as well as all my other family members and friends for their support in my research and education.

ACKNOWLEDGEMENTS

I would like to thank Luke Pangle for his guidance, mentoring, and his accessibility. I also would like to thank Brian Meyer and Rebekah Chapman for their advice and role on my committee, their role was crucial in the completion of this thesis. I would like to thank Luke Pangle, the Department of Geosciences at Georgia State University, the Cleon C. Arrington Research Initiation Grant Program, and the American Institute of Professional Geologist for funding my research and education.

I would like to express appreciation to Till H.M. Volkmann out of the University of Arizona- Biosphere 2 for the countless hours of advice and assistance he gave in this research. I would like to extend appreciation to Richard Milligan, Brent Aulenbach, Jeff Riley, Lanier Henson, Nate Rabideaux, Sam Mutiti, Doug Oetter, Mary & Tobin Hart, my course instructors, and many others for their help and support.

TABLE OF CONTENTS

LIST OF TABLES

LIST OF FIGURES

1 TOWARD A DIFFUSIVE, NON-DESTRUCTIVE APPROACH TO MEASURING STABLE ISOTOPES OF WATER WITHIN TREE STEMS

1.1 Introduction

In most tropical and temperature environments, evapotranspiration represents the largest annual flux of water from landscapes. The biologically mediated process of transpiration constitutes more than half of total evapotranspiration at continental and global scales (Good, Noone and Bowen 2015; Maxwell and Condon 2016; Schlesinger and Jasechko 2014) though notably, some of the estimates in these cited works remain contradictory. The range of these estimates makes transpiration one of the more difficult variables to account for when creating a model of the global water cycle. These facts highlight the importance of understanding how transpiration—and the subsequent impacts of dynamic transpiration on other water flows—respond to environmental change. Toward that aim, a persistent obstacle is the limited availability of measurement techniques that allow temporally-resolved observations of soil-water uptake by plant roots—the source of water acquisition that drives transpiration.

Traditional methods for documenting the spatial and temporal dynamics of root uptake utilize the stable isotopes $\delta^{2}H$ and $\delta^{18}O$. The traditional methodology involves destructive sampling of cylindrical sections of xylem cells from tree stems, or whole branches removed from the canopy. Liquid water is extracted from the plant tissue via cryogenic distillation (McCarroll and Loader 2004). This destructive methodology limits the temporal resolution, and duration, of sampling. Subsequent core extractions will eventually kill the tree being sampled.

More recently, workers have established isotopic equilibrium between wet samples and controlled airspace, then measured the isotope composition of the resulting vapor (Munksgaard, Wurster and Bird 2011; Orlowski, Pratt and McDonnell 2016b; Koehler and Wassenaar 2011).

The premise behind this method is that these controlled volumes of airspace are in equilibrium. Equilibrium is defined as a net exchange of zero water molecules between phases and a net exchange of zero isotopes between phases. The isotopic ratios of the vapor within the volume can be used to calculate the isotope composition of the liquid water knowing the temperature at the site of exchange, and with the knowledge that the gas and liquid were in equilibrium, indicative of the isotopic ratios of the liquid water. Workers have demonstrated how this liquid-vapor equilibration approach could be utilized for *in situ* sampling of stable-isotope ratios in both soil-water and water within tree stems (Volkmann et al. 2016; Volkmann and Weiler 2014). This represents a significant advance, although their approach requires a highly technical, and expensive, gas-conveyance system that cannot be readily duplicated by many research groups.

We validated the efficacy of a novel liquid-vapor equilibration technique for monitoring stable-isotope ratios of xylem water across tree species with varying xylem architectures and cell density, basing our method on the principles of diffusion. Isotopic equilibrium between liquid source and emanating vapor occurs rapidly in coarse-textured soils, and possibly in plant tissues (Koehler and Wassenaar 2011; Volkmann and Weiler 2014). We attempted to verify the timescales required to reach isotopic equilibrium across a range of tree species using the proposed technique. We hypothesized that the effects of different xylem-cell architectures and its effect on vapor diffusivity, coupled with differences in xylem-sap composition would cause equilibration times, and measurement accuracies to differ**.** We applied the methodology to different tree species to determine if problems would arise among its use across a variety of species. Species included *Pinus taeda* (L.), *Oxydendrum arboreum* (L.), *and Fagus grandifolia* (Ehrh)—all common in forests of the eastern US, including angiosperms and a gymnosperm, and spanning a range of wood density. We quantified the time required to achieve isotopic

equilibrium within the sample airspace. Isotopic equilibrium was confirmed by demonstrating that the correct liquid-water isotope composition (reservoir water composition) can be recalculated (Munksgaard, Wurster and Bird 2011; Orlowski, Pratt and McDonnell 2016b; Koehler and Wassenaar 2011).

1.2 Literature Review

1.2.1 Role of Transpiration in Evapotranspiration

In hydrology, water loss from the land and ocean surface to the atmosphere is collectively described as evapotranspiration (ET). Evapotranspiration consists of two distinct processes, the biologically controlled process of plant transpiration (T), and the physically controlled process of water evaporation (E). It is difficult to constrain the exact proportions that each of these processes contributes to the combined evapotranspiration amount (Fetter 2000). Obviously, these proportions are locale-specific; different areas will have different amounts of evaporation and transpiration dictated by land coverage. The amount, type, and concentration of vegetation along with the percentage of impervious surfaces in the area all influence the levels of E and T. Partitioning T and E in different environments has been a research interest for decades (Allen et al. 1998; De Graaf and Van den Ende 1981; Fritschen and Shaw 1961; Liu, Zhang and Zhang 2002).

Recent work has been done to constrain the proportion that transpiration contributes to evapotranspiration as it relates to global climate and water cycle models. Knowledge of that proportion gives workers a baseline to use when modeling changes to transpiration caused by environmental change. Jasechko et al. (2013) report that the mean-global proportion of T/ET is greater than 80%. In response to Jasechko et al. (2013), Coenders-Gerrits et al. (2014) argue that this is a gross overestimate and that mean-global T/ET is more on the order of 35-80%.

Coenders-Gerrits et al. (2014) claim that the parameterization used to model runoff in Jasechko et al. (2013) was too low, resulting in a much higher transpiration value. In response, Jasechko et al. (2013) suggest that the use of H and O isotopes in the future could help refine the model parameters used to estimate T/ET percentages.

The following year, Schlesinger and Jasechko (2014) report that the mean ecosystem-scale estimate of T/ET is at 61% ± 15%, well below the value reported by Jasechko et al. (2013) the previous year. Good et al. (2015) found a global range of 56 to 74% as the fraction of T/ET, with a mean value of 64%. Maxwell and Condon (2016) suggest a range of T/ET estimates of 50 to 74%, with a mean value of 62%. On a more local scale, Brunel et al. (1997) found that T only contributed about 20% of total ET during a plot-scale study in the Republic of Niger, well under the global mean estimate. This is a huge range of values. Workers have global mean T/ET estimates ranging from 20% to greater than 80%, with estimates large and small in between. The uncertainty associated with these measures drives the need to develop methods that allow direct measurements of soil-plant-water interactions that are key to understanding the dynamics of ET.

1.2.2 Use of Stable Isotopes in Ecohydrology

Stable isotopes have long been used to make inferences and observations about the natural world and soil-plant-water interactions (Peterson and Fry 1987; Ehleringer and Dawson 1992). In ecohydrology, the different oxygen and hydrogen isotopes in water molecules have been used to elucidate soil and root interactions, as well as to give providence and age to waters (Dansgaard 1964). Comparing the stable isotope composition in different waters allows workers to quantify fractional contributions of different water sources to some composite flow of interest, such as streamflow. These compositions could be the naturally occurring ratios, or they could be

the ratios after introducing a labeled water into the system that has distinctive isotopic composition.

Isotopic values of the hydrogen and oxygen atoms in water molecules are referred to throughout this work in the δ-notation, which provides the ratios of heavy to light isotopes present in a given sample of water, relative to an international standard. The equations below describe this ratio.

$$\delta^2 H = [\frac{(^2H/^1H)_{sample}}{(^2H/^1H)_{standard}} - 1\ ] * 1000$$

$$\delta^{18} O = [\frac{(^{18}O/^{16}O)_{sample}}{(^{18}O/^{16}O)_{standard}} - 1\ ] * 1000$$

These values are given in the unit parts per thousand (‰), or per mil and can refer to the liquid or vapor phase of a water.

In thermodynamic reactions (i.e., phase changes between liquid and gaseous water), differences in molecular energies and concentration gradients cause isotopes of the same element to disproportionately accumulate on one side of the reaction. That disproportionate accumulation is described by a fractionation factor, α, which can be used to estimate the accumulation or depletion of a certain isotope on either side of a reaction. Under equilibrium conditions, fractionation occurs primarily in two different ways, either as physicochemical fractionation or as diffusive fractionation. Physiochemical fractionation can occur under equilibrium or non-equilibrium conditions, and is based on the bond strength formed by the isotopes. This bond strength is dictated by the molecular weight of the isotopes; heavier isotopes will have stronger bond strengths within the molecule compared to the lighter isotopes (Clark & Fritz 1997). More energy is required to induce a phase change with heavier isotopes, causing lighter isotopes to change phase quicker. Because the heavier isotopes take longer (require more energy) to change

phase, they tend to be preferentially concentrated in the denser phase (more will be present in liquid water than the resulting vapor).

For water isotopes in equilibrium conditions, fractionation factors can be easily estimated based on the temperature at the site of a phase change (see Horita & Wesolowski 1994; Majoube 1971). In non-equilibrium conditions, kinetic fractionation can occur, which makes it much more difficult to estimate fractionation factors in a reaction. Changes in temperature or changes made to reactant amounts can cause changes to the mass-dependent nature of physiochemical fractionation heightening, or lessening its effect (Clark & Fritz 1998). The exact influence is hard to know, making kinetic fractionation a process a difficult to parameterize.

For water, it is key to understand the fractionation relationship between liquid and water phase changes. When a volume of liquid water undergoes evaporation, a change from liquid water to water vapor, two fractionation processes are at play. The liquid water undergoes a depletion in the lighter isotopes (^{16}O and ^{1}H), while the resulting vapor will have an enrichment in light isotopes. At the same time, the liquid water is experiencing an enrichment in heavier isotopes (^{18}O and ^{2}H) relative to the remaining proportion of light isotopes because the lighter isotopes are preferentially moving to the vapor phase.

One of the major benefits of tracing water use in plants via stable isotopes is that water uptake and movement through xylem structures on the interior of the plant is a non-fractionating process (Ehleringer and Dawson 1992; White *et al.* 1985). Once water is taken up through the roots, the isotopic signature of heavy to light water isotopes does not change as water is transported through the stem. Evaporative enrichment of that water will occur at areas of water loss, like at leaves where there is transpiration water-loss, or through exposed sapwood. If the water in xylem can be analyzed prior to any of these evaporative processes occurring, then the

measurement will be an integrated measure of general water uptake location (depth and zone) (Ehleringer and Dawson 1992).

Isotope ratio mass spectrometry (IRMS) has been the traditional way to measure $\delta^{2}H$ and $\delta^{18}O$ isotope ratios, but in recent years the development of isotope ratio infrared spectroscopy (IRIS) has taken over as a precise and reasonable alternative (Ehleringer, Roden and Dawson 2000; Gupta et al. 2009). IRMS has the downside of being costly, with intensive time investments in water extraction and sample preparation (Zhao et al. 2011). IRIS offers a lower per-sample cost, as well as minimal time investment in sample preparation.

Tree xylem water still requires an extraction method regardless of the analytical approach employed. Destructive sampling of xylem cells is typically required, then different time-intensive processes of extracting the liquid water that is within the solid cell structure of the xylem is required. Contemporary laser spectrometers are able to receive steady inflows of water vapor from a gas sample (rather than volatilizing a discrete liquid sample), and measure ratios of $^{2}H:^{1}H$ and $^{18}O:^{16}O$ at a frequency greater than 1 Hz, although acceptable precision usually requires averaging over at least a few seconds. This new measurement capability has laid the ground work for studies employing liquid-vapor equilibration techniques as a way to estimate the isotope ratios in liquid water without actually having to extract the water from the porous media (Munksgaard, Wurster and Bird 2011; Orlowski, Pratt and McDonnell 2016b; Koehler and Wassenaar 2011; Oerter et al. 2017).

1.2.3 Water Extraction Techniques

There are a number of techniques used to remove water from soil and organic matrices each with its own intricacies. Orlowski (2016b) did an extensive review of these methods and presented a significant overview of the prevalent methods, as well as their benefits and

shortcomings. In an ecohydrological context, there are roughly 5 techniques which get the most use: cryogenic vacuum distillation, centrifugation, mechanical squeezing, direct vapor equilibration, and microwave. Tables 1 and 2 further below give a review of some ecohydrological studies and the extraction method used.

Cryogenic vacuum distillation separates the liquid water by bringing samples to high temperatures at vacuum pressures, and then distilling out the condensate using liquid nitrogen (Orlowski 2016a). Centrifugation spins samples at high velocities, separating the liquid water from the sample. Mechanical squeezing uses hydraulic presses and specially designed metal chambers to physically press liquid water out of samples for analysis (Orlowski 2016b). Direct vapor equilibration uses the principles of isotopic and thermodynamic equilibrium on a controlled airspace and the sample. The resulting vapor, in isotopic equilibrium, can them be distilled out, or the vapor directly measured. Microwave extraction is similar to direct vapor, but the irradiation allows a greater portion of liquid water to be extracted (Munksgaard et al. 2014)

1.2.4 Temporal Resolution of Xylem Water Sampling

The temporal resolution of xylem water isotope sampling in field environments is steady throughout many studies. A review of 20 studies employing a variety of extraction and sampling techniques was completed, the sampling regime and frequency is shown below in Table 1. These studies, ranging from Dawson (1993) to McCutcheon et al. (2017) all have comparatively similar sampling frequencies. 14 of the 20 studies (70%) are less than 100 days in length, and of those 14, 11 of them have a total of 15 or fewer samples for the duration of their studies. Of the 6 studies greater than 100 days in length, two of the studies McCutcheon et al. (2017) and Gaines et al. (2016) make assessments using the same dataset. The third study greater than 100 days in

length, Koeniger et al. (2010), had 3 total samples throughout the entire duration of a 200-day study.

The remaining 11 studies averaged 23 days in length, with an average total number of xylem water samples taken at 9.7. This would come out to be just under 1 sample every other

Table 1 Review of ecohydrological studies which sample xylem water. Sampling frequency, extraction method, and analytical methods are all noted when that information was available.

Author	Duration of Study (days)	Sampling Frequency (days)	Total Number of Samples	Extraction Method	Analytical Method
(McCutcheon, McNamara et al. 2017)	730	1 sample per 5 days	155	Cryogenic Vacuum Distillation	IRIS
(Piayda, Dubbert et al. 2017)	12	5 samples per day	60	Cryogenic Vacuum Distillation	IRIS
(Gaines, Stanley et al. 2016)	1095	1 sample per 18 days	60	Cryogenic Vacuum Distillation	Gas Chromatography, Hot Chromium Reaction, IRMS
(Schwendenmann, Dierick et al. 2010)	30	Days: 0.5, 1, 2, 7, 22, 25	6	Cryogenic Vacuum Distillation	IRIS
(Koeniger, Leibundgut et al. 2010)	200	Days: 150, 186, 197	3	Azeotropic Distillation	IRMS
(Lambs and Saenger 2011)	16	1 sample per 3 days	5	Headspace Equilibration	IRMS
(Beyer, Koeniger et al. 2016)	10	1 sample per day	10	Cryogenic Vacuum Distillation	IRIS
(Meinzer, Brooks et al. 2006)	70	Days 1-7: Daily Days 8-70: 1 sample per 10 days	14	Cryogenic Vacuum Distillation	IRMS

Table 2 Continued review of ecohydrological studies which sample xylem water. Sampling frequency, extraction method, and analytical methods are all noted when that information was available.

Author	Duration of Study (days)	Sampling Frequency (days)	Total Number of Samples	Extraction Method	Analytical Method
(Brunel, Walker et al. 1997)	12	1 sample per day	12	Azeotrophic Distillation	-
(Schwinning, Davis et al. 2002)	16	Days: -7, 0 7	3	Cold Trapping	IRMS
(Williams, Cable et al. 2004)	15	1 sample per day	15	Cryogenic Vacuum Distillation	IRMS
(Gaines, Meinzer et al. 2016)	42	Week 1: Daily Week 2: 3 samples per week Week 3: 2 samples per week After Week 3: 1 sample per week	14	Cryogenic Vacuum Distillation	IRMS
(Marc and Robinson 2004)	12	1 sample per day	12	-	IRMS
(Volkmann, Kühnhammer et al. 2016)	11	Continual	N/A	N/A	IRIS
(Yepez, Huxman et al. 2005)	15	2 Samples on Days: -1, 1, 3, 7, 15	10	Cryogenic Vacuum Distillation	IRMS
(Kalma, Thorburn et al. 1998)	17	Days: -1, 0.5, 1, 4, 8, 17	6	Azeotropic Distillation	IRMS
(Brooks et al. 2009)	420	96 samples Days: 1, 360, 420	288	Cryogenic Vacuum Distillation	IRMS
(Evaristo et al. 2015)	-	-	1460	264 Samples: Azeotropic Distillation 1079 Samples: Cryogenic Vacuum Distillation 112 Samples: Liquid-Vapor Equilibrium	-
(Dawson 1998)	1095	Monthly	75	Cryogenic Vacuum Distillation	IRMS
(Dawson 1993)	7	Days: -3, 1, 3	-	Cryogenic Vacuum Distillation	IRMS

day of the study. Brooks et al. (2009) collected 288 samples over a 420-day period, whereas Dawson (1998) had 75 samples over the course of 1,095 days. Evaristo et al. (2015) was a review paper aggregating sample data from many studies. One outlier in this study review was Volkmann et al. (2016) who was able to continuously monitor xylem water over the course of an 11-day study. The temporal resolution and innovative sampling technique employed by Volkmann et al. (2016) is one of the reasons behind the effort to build off their work.

1.2.5 Ecohydrological Water Extraction Techniques and Development

Beyond the analytical method used to measure relative abundances of water isotopes, the approach to extract liquid or vapor samples of soil, xylem, or other water trapped in a matrix has its own complexities. Tables 1 and 2 display the extraction and analytical techniques employed to test soil, xylem, and vegetation water. Note the heavy reliance on cryogenic vacuum distillation for extracting pore and xylem water. Azeotropic distillation is another method for extracting water that has historically been used in water extraction. Lambs and Saenger (2011) employ a headspace vapor equilibration technique which directed equilibrated vapor into a continues flow IRMS.

Beyond the work that has been done to explore these extraction methodologies in ecohydrological studies, others have done work directed more on just method development, with the most recent focus being direct liquid-vapor equilibration techniques. It is based off temperature-dependent fractionation factors of oxygen and hydrogen isotopes as described in previous sections. In meteoric waters, the relationship between oxygen and hydrogen isotopes within a water molecule is shown below.

$$\delta^{2}H = 8.2 * \delta^{18}O + 11.27$$

This is based on a global mean isotopic composition of precipitation, and is called global meteoric water line (GMWL), with the empirical relationship well established (Rozanski 1993). Water samples plotted against this function show if they are experiencing isotopic depletion or enrichment relative to the GMWL, which would indicate some of the physical processes acting on the source. Direct liquid- vapor equilibration techniques use well-established temperature-dependent isotopic fractionation factors of ^{18}O and ^{2}H to calculate the isotopic composition of the liquid or vapor pool if the composition of the other pool is known (Majoube 1971; Horita and Wesolowski 1994). In this case, you are inferring the liquid isotopic composition based off composition of vapor in isotopic equilibrium with the liquid source water. Below shows the formula used for calculating the fractionation factors for $\delta^{18}O$ and $\delta^{2}H$ between liquid and vapor reservoirs.

$$10^3 \ln \alpha_{l\text{-}v} (^2H) = 1158.8 (T^3 / 10^9) – 1620.1 (T^2 / 10^6) + 794.84 (T / 10^3) – 161.04 + 2.9992 (10^9 / T^3)$$

$$10^3 \ln \alpha_{l\text{-}v} (^{18}O) = -7.685 + 6.7123 (10^3 / T) – 1.6664 (10^6 / T^2) + 0.35041 (10^9 / T^3)$$

Direct liquid-vapor equilibration techniques came into prominence as a potential research topic with the publication of Koehler & Wassenaar (1999), and Hsieh et al. (1998). Koehler & Wassenaar (1999) measured $\delta^{18}O$ and $\delta^{2}H$ of the water contained within geologic material used a modified CO_2 liquid water equilibrator with soil samples attached, to pump the vapor samples into an IRMS for analysis. This built off the method Hsieh et al. (1998) came up with previously. Others have used a comparable setup but used helium as their carrier gas, not CO_2 (Rübel et al. 2002). Wassenaar et al. (2008) built off of this technique, and came up with a similar technique that could be used on an off-axis integrated cavity output spectroscopy device (OA-ICOS, a form of IRIS). In this instance, Wassenaar et al. (2008) were sampling the head

space of a perceived gas-impermeable Ziploc freezer bag containing wet soil samples. Further on this line of research, Koehler and Wassenaar (2011) demonstrated the stability of direct and continuous monitoring of the head-space equilibration method using a commercially available wavelength-scanned cavity ring down spectroscopy (WS-CRDS).

Most recently, researchers have used vapor permeable membranes to allow vapor to diffusion through membrane-covered sensors which route the vapor to some commercially available IRIS analytical system for measurement (Oerter et al. 2017; Volkmann et al. 2016, Rothfuss et al. 2015; Gaj et al. 2016). Much of this development around vapor-permeable membranes stems from the work of Munksgaard, Wurster and Bird (2011) who developed an IRIS auto-sampling device for liquid water based around expanded polytetrafluoroethylene (PTFE) tubing, a vapor-permeable material. This PTFE tubing approach was what was designed and used in Volkmann and Weiler (2014) for their soil sensor, as well as their future xylem water isotope probe Volkmann et al. (2016).

1.2.6 Problems with Traditional Extraction Methods

1.2.6.1 Cryogenic Vacuum Distillation

The major water extraction method for soil and vegetation water in stable isotope hydrology, cryogenic vacuum distillation, has been under scrutiny over the last few years over concerns about the reliability of the method, specifically in its ability to extract soil water. Problems associated with cryogenic vacuum distillation have been known for the last two decades, but only recent work has delved into the mechanistic explanations behind the problems. Brooks et al. (2009) reported some of the issues associated with extraction of bound soil waters. Isotopic signatures of the same soils, one extraction via suction lysimeter, the other extraction via cryogenic vacuum distillation, showed differences. While they were different, this is not

necessarily surprising as there is a major difference between the two methods. Cryogenic distillation extracts all of the bound water, whereas suction lysimeters are only extract a fraction of the total bound soil water. Orlowski et al. (2013) performed a replicated experiment using isotopically-labelled waters in different soils, and the cryogenically extracted waters differed from the known composition in a number of the soil types. In a review of soil extraction methods, Orlowski, Pratt and McDonnell (2016b) found that cryogenic extraction was less precise than mechanical squeezing, or centrifugation of pore water. While less precise, Orlowski et al. (2016b) still found direct vapor equilibration to be a viable method, though in regard to IRIS some concern needed to be paid to influence of organic compounds. Across all studies, workers found that water extraction in heterogeneous soils made cryogenic extraction more difficult. Additional problems arise in the lab to lab comparisons of cryogenic distillation methods. Extraction duration, pressure, and temperature differences between labs can make it difficult to compare inter-lab results (Orlowski, Breuer and McDonnell 2016a).

These problems associated with cryogenic vacuum distillation as they relate to soil could have implications on cryogenically distilling plant water. Similar processes influence water extraction from plant tissues and xylem structure as would influence water extraction for soils. Heterogeneity in the plant issue densities, xylem architecture, or in other structural components of plants could make bound water more difficult to extract, or as is the case when cryogenically extracting soil water, some components of the plant water that is more tightly bound. Another confounding factor is the potential for high concentrations of terpenes and other volatile organic compounds throughout the heartwood and sapwood of trees (Roffael 2006).

1.2.6.2 Considerations for Isotope Ratio Infrared Spectroscopy

Laser-based spectroscopy is prone to interference from a number of different avenues of contaminants and physical parameters. These instruments measure the absorbance of a laser after it strikes a molecule, and depending on the frequency of the absorbance; you can infer the isotope of the specific element in question. For our research, we are interested in $^{18}O/^{16}O$ relationships, as well as $^{2}H/^{1}H$. When water is volatized into a continues flow IRIS isotope analyzer, there are also relationships between the concentration of water in the air stream relative to other ambient atmospheric gases (Kurita et al. 2012). If water molecules are highly concentrated, or minimally, this can influence the integrated absorption measurement of ^{18}O and ^{2}H frequencies. Though well-established, these relationships are likely instrument specific. Similarly, if volatile organic compounds from the organic matter the water is extracted from enter the analytical column, they can absorb at similar frequencies from the laser measures or cause types of spectral contamination skewing results and limiting accuracy (Chang et al. 2016).

1.2.7 Timescales Required for Equilibration

Two physical processes that are important to know in regard to liquid-vapor equilibration techniques is the time required to reach isotopic and thermodynamic equilibrium. In the development of a new, or improved methodology for direct liquid-vapor equilibration knowledge of the time required equilibration will be integral in understanding if it has improved temporal resolution in sampling. In applying Majoubes equation to calculate the isotope composition of the liquid or vapor of a water, one of the constraining factors is that the vapor and liquid need to be in isotopic equilibrium, as well as thermodynamic equilibrium. Unless these parameters are met, the associated fractionation factors used to convert ^{18}O and ^{2}H values cannot confidently be applied. Horita and Wesolowski (1994) show the time required to reach these equilibrium levels

at a varying degree of temperatures. These times were on the order of 31 hours to 101 hours. Wassenaar et al. (2008) do not report the time required for their Ziploc bagged samples to reach 100% relative humidity and isotopic equilibrium, but do mention the bags are gas impermeable on the scale of a number days. Oerter et al. (2017) report that in their bagged-soil direct vapor equilibration method, saturated soils are left to equilibrate for 12 hours and 22° C. Munksgaard, Wurster and Bird (2011), Koehler and Wassenaar (2011), Volkmann et al. (2016) use continuous flow controls allowing for management of isotope and humidity concentrations in the flow stream prior to entry into the analytical instruments inlet. Their probe crates a pressure gradient from the outside of the probe to the inside of the probe; this allows vapor flow into the probe based on advection, a non-fractionation process. The foundations of this process assume that vapor on the outside of the probe was already in equilibrium with the liquid-water. In their case, this equilibration time is not as pressing of a background measurement.

1.3 Project Overview

We tested our proposed sampling method on excised tree segments from common tree species in the southeastern United States. These tree segments were stored in vapor-sealed containers, filled partially with isotopically distinct waters. Chambers were installed onto these segments that would allow for diffusion to occur between the liquid xylem water and the headspace in an attached container. Isotopic measurement of the diffused vapor allowed the application of empirical equations that back-calculate the isotopic composition of the liquid xylem water.

Validation of vapor isotopic measurements due to day to day changes in the function of the laser spectrometer required the samples to be run against standards. Laboratory conditions limited accessibility to a gas-nebulizer, a device used in the calibration of commercially available

laser spectrometers. A method to analyze standards at a known water vapor concentration, with a known isotopic composition had to be devised in order for cross-comparisons between analytical runs to be possible.

The feasibility of the diffusive sampling method was implemented across a range of tree species and was additionally applied across different water vapor concentrations. Identification of any specific species that could pose problems were identified, and the ideal water vapor concentration range was identified.

1.4 Methods

1.4.1 Sapling Set-up & Validation of Xylem Flow

We utilized cut saplings to implement our sampling design on multiple tree species. Tree segments, or saplings, are known to still conduct water through the xylem cells (Čermák et al. 2007). Laboratory based studies utilizing cut saplings have a history of use in the tree physiology realm of research (Teskey, Hinckley and Grier 1983). We utilized saplings of varying wood densities and xylem architectures, as well as angiosperms and gymnosperms. One or two stem segments from each of 3 different species were utilized to test our approach, ranging in length from 50.5 cm to 80 cm in length, and from 4.5 cm to 7.5 cm in diameter. Species included *P. taeda, O. arboreum, and F. grandifolia*— all of which are tree species that occur commonly in the southeastern United States. These tree segments were placed in buckets containing deionized

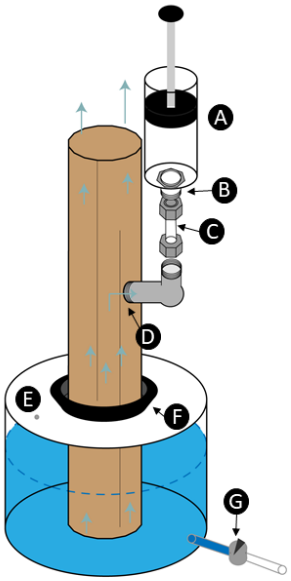

Figure 1 Laboratory set-up of sapling & bucket
(A) Air-tight gas chromatography syringe (B) ½" Swagelok bulkhead fitting (C) FEP connection with Swagelok connectors (D) 90° Swagelok elbow fitting (E) Venting port (F) Gas-tight stopper surrounding sapling (G) Outlet port for liquid reservoir

water with a known isotope composition. These buckets contained a venting hole on the top (1/64”), and a valved outlet port on the bottom for continued testing of the liquid water in the reservoir throughout the experiment (See E, Figure 1). Figure 1 above shows a schematic diagram of how the saplings are setup in the buckets. Figures 2 and 3 show a full, step-by-step description of the physical sampling set-up, sampling procedure, and quality control and assurance.

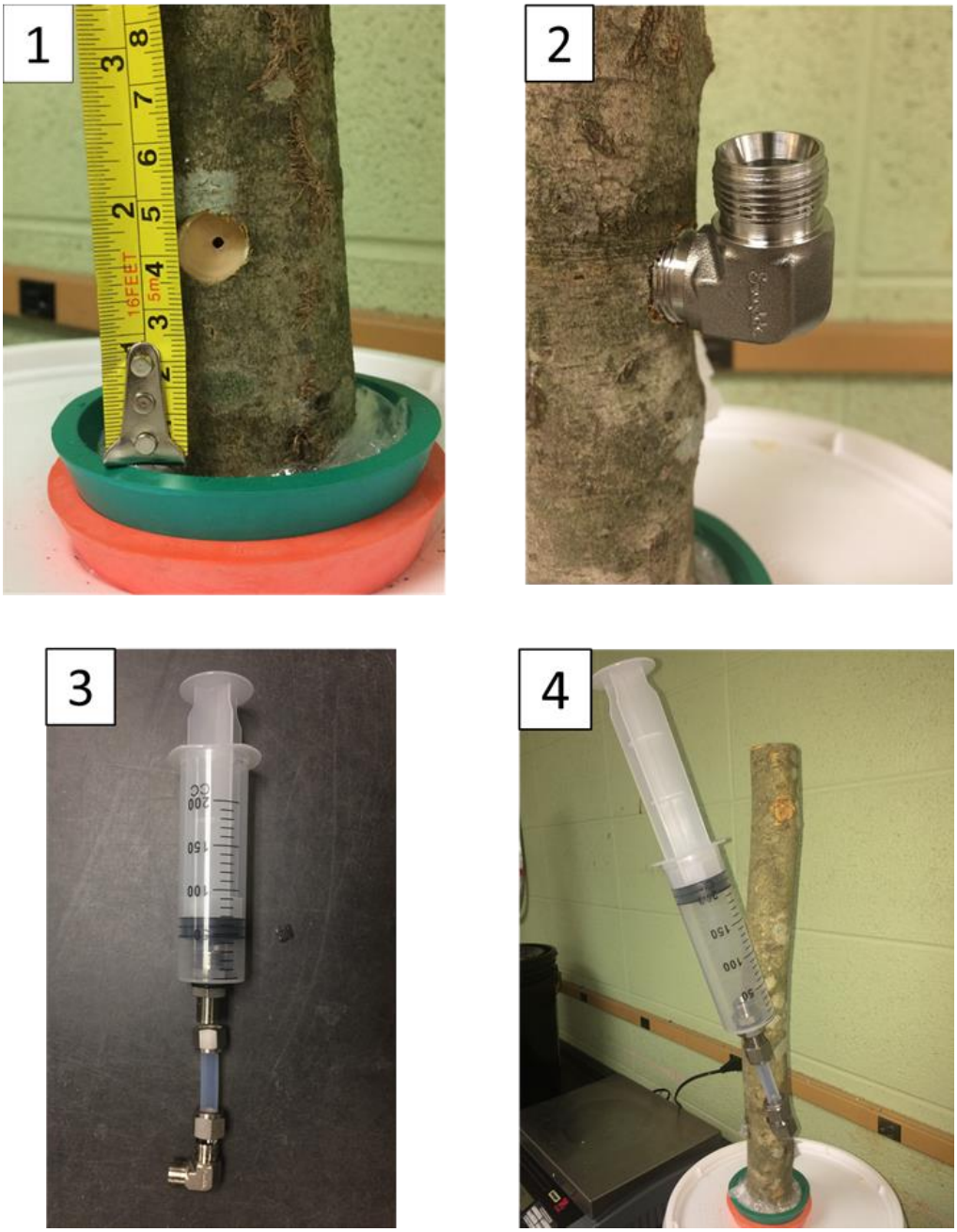

Figure 2 Picture description of physical sapling set-up

(1) A large diameter (<1/2") borehole is drilled into the sapwood of a sapling or tree to an appropriate depth depending on the tree or sapling size. Within the large diameter borehole, a second whole is drilled using a 3/16" (2) Large diameter (1/2" or ¾") stainless steel Swagelok 90° elbows are screwed into the boreholes previously drilled. (3) Swagelok fittings are attached to small amounts of polyethylene tubing that have thick wall and connected to a Swagelok-adapted 175 mL syringe. (4) The 175mL syringes filled with N_2 calibration gas and attached to the tree sapling through the Swagelok connected tubing.

Figure 3 Picture diagram of sampling procedure and analysis

(5) The equilibrated syringes are injected into a 2-Liter Supelco Inert Foil Gas Sampling Bags. (6) A 1-liter, acrylic Hamilton Super Syringe, designed for gas sampling is filled with N_2 calibration gas (7) Calibration gas is injected into the gas sampling Bag containing to the vapor sample of the xylem water (8) The Supelco bag is left to mix for 10 minutes before it is attached to the gas intake on the LGR-IWA-45EP. (9) Standard removal, follows steps 5-8 prior to analysis

With these setups, theoretically, the only exit point for water vapor should be through the sap flow exiting through the exposed xylem at the top of the tree segment. These saplings were sealed into the buckets with commercial silicone sealant, or with a rubber stoppers. To ensure the

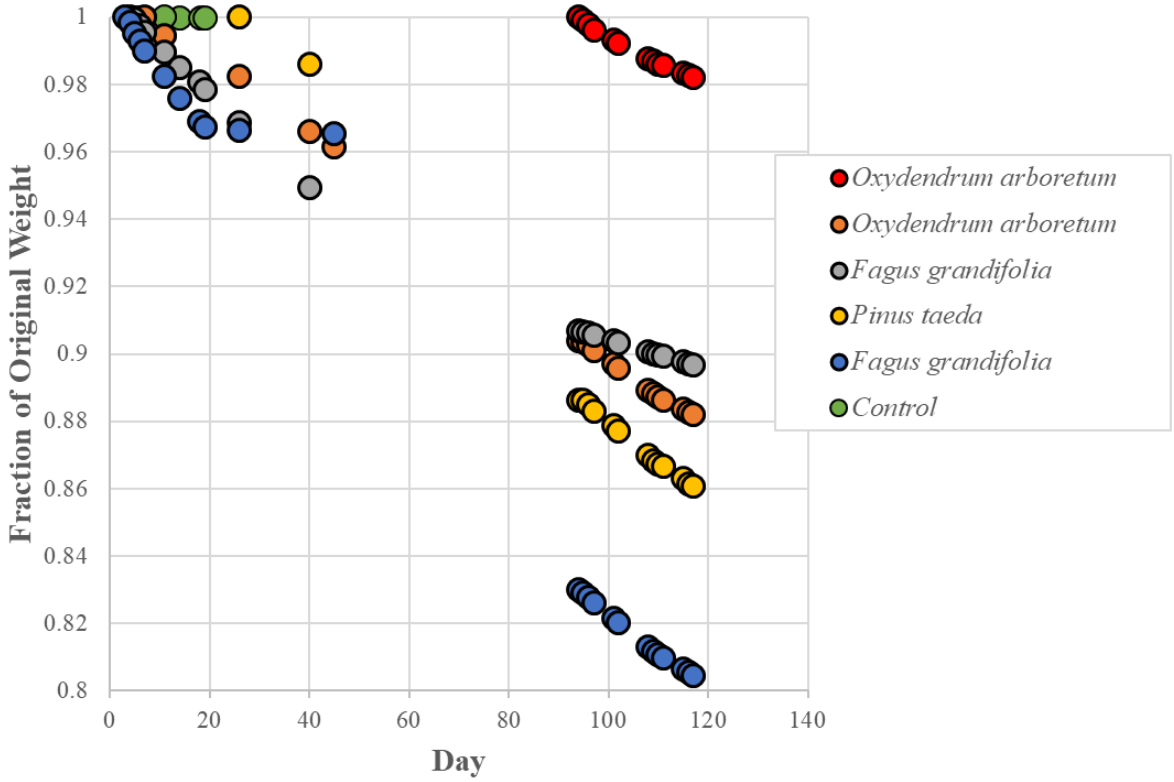

Figure 4 Sapling mass loss throughout experimental period, shown as a portion of the original mass. Two O. arboreum, two F. grandifolia, and one P. taeda were used to test the methodology.

seal of these buckets, a control was setup with the same outlet port and venting hole as the sapling buckets. The control bucket was filled with a set amount of water, and then weighed throughout the sampling period to determine if there was any mass-loss of the water, which would be indicative of evaporation from the chamber. Similarly, to ensure the trees were still moving water up through their stems, the saplings and the buckets of water were measured throughout the experiment. Mass loss in this instance is associated as the water lost from xylem sap flow. Figure 4 above displays the mass loss associated with the control, as well as each individual sapling throughout the course of the study. Measurements of the control bucket were

ended when it became clear there was no water loss due to leaks in the buckets, or through the venting port.

Ports were placed into each of the saplings, via large diameter (1/2 in.) boreholes drilled through the phloem and cambium, into the sapwood of the trees [see (1) Figure 2]. A much smaller diameter hole (3/16 in. to 1/64 in.) was drilled radially into the heartwood of the tree segments. Stainless Steel Swagelok ½ in. 90° elbows were screwed into the sapwood of each of the larger diameter boreholes, a thermocouple wire was threaded along the side of this fitting so that the temperature at the boundary layer between the liquid and vapor is definitely known (Figure 5). These components were then sealed externally with commercial silicone. Figure 5 displays the placement of the ports onto the sides of each sapling.

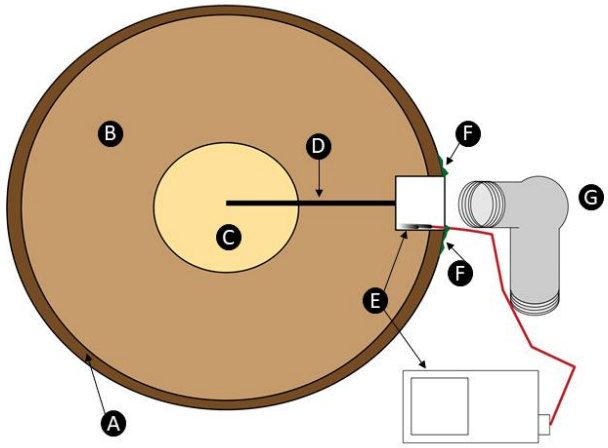

Figure 5 Cross-section of sampling port
(A) Bark and cambium (B) Sapwood (xylem) (C) Heartwood (D) Small diameter hole extending into heartwood (E) Thermocouple wire and display device (F) Commercially available silicone sealant (G) 90° Swagelok elbow

This set-up was thought to be air-tight enough to limit any evaporative fractionation that could occur from leak points around these fittings. High-capacity polyvinyl chloride (PVC) syringes (175 mL) were fitting with Swagelok bulkhead fittings that allow for connection to the Swagelok 90° elbow either through a 1/2 in. diameter, high density polytetrafluoroethylene (PTFE) piece of tubing (Figure 6). Alternatively, this connection could be made via a male to male stainless-steel Swagelok connector, though these fittings are cost prohibitive, female Swagelok

tubing connections are much cheaper. PTFE has very low sorption rates, and works as a diffusive barrier well for the proposed purpose (Parker and Ranney 1994). While the syringes had a total volume of 200 mL, because of the bulkhead fitting on the interior of the syringe, the plunger could not fully actuate, leaving around 25 mL of dead space at the head of the syringe. See Figure 6 for a schematic diagram of these connections.

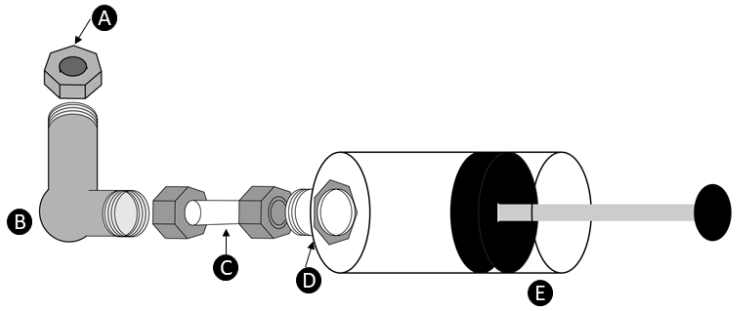

Figure 6 Diagram of sampling syringe and connection port
(A) Swagelok cap (B) 90° Swagelok elbow (C) FEP connection with Swagelok connectors (D) ½" Swagelok bulkhead fitting (E) PVC syringe

1.4.2 Sampling Procedure

Once the chambers were installed and sealed onto the saplings, the fittings were flushed with N_2 calibration quality gas. The PVC sampling syringe was then filled with more of the N_2 calibration gas, and then attached to the Swagelok elbow serving as the port on the tree segments [see (4), Figure 2]. These syringes were left attached to the saplings so that the liquid water within the xylem exposed on the interior of the port comes into isotopic and thermodynamic equilibrium with the gas air space within the syringe and tubing. This N_2 calibration gas is devoid of all water vapor, which means there should be no isotopic mixing of water vapor occurring, whether that be from water vapor present in the ambient air, or from another source. Syringes were considered to be at isotopic and thermodynamic equilibrium when the relative humidity within the interior of the syringe reached 100%. Without exposure to the liquid constrained to the xylem cell, the N_2 calibration gas theoretically has a relative humidity at 0%, as there should be no water vapor present.

Approximations were made of the time required to reach equilibrium for both sample extraction, and for the standard curve corrections. A handheld psychrometer (OMEGA Engineering-HHAQ-106), was used to make these measurements in both cases. For the syringes attached to the tree segments, the plunger was removed and the psychrometer was placed into the syringe with a rubber stopper. A separate Swagelok 90° elbow was connected to the syringe and the entire apparatus was flushed with N_2 gas. A small drop of water, (< 1 mL) was placed into the exposed end of the Swagelok elbow and then capped off. The time elapsed for the psychrometer to reach 100% relative humidity was noted.

After leaving the syringes attached to the saplings overnight, the syringes were detached. They were capped with a Swagelok cap at the end, and then injected into collapsible volume bag

for dilution. The bags used were 2-liter Supelco™ Inert Foil Gas Chromatography Sampling Bags (Sigma-Aldrich, Inc., Merck KGaA, Darmstadt, Germany). These bags are thought to be gas-impermeable and diffusion resistant for the timescales of our use (< 1 hour). The samples of xylem vapor are slowly injected into the bags at a rate of around 2.917 mL/sec. An acrylic, Hamilton 1-L Super Syringe designed for gas sampling was filled with a set volume of the N_2 calibration gas and injected in the Supelco sampling bag along with the sample volume. This was to bring the 100% RH vapor sample down to a humidity level that could be replicated across all the samples and the standards. The injection of the dilution gas occurred at a comparable rate as the sample, with some variability due to manual actuation of the syringe [see (5) - (7), Figure 3]. For each of the three tree species, we tested vapor samples at three different amounts of dilution gas, 400 mL, 600 mL, and 800 mL. These dilution volumes represented water vapor mixing ratios ranging from 8,000 parts per million volume (ppmv) to 9,800 ppmv.

Following injection of the dilution gas, the Supelco sampling bags were left to sit between 10-25 minutes. Allowing the bags to sit for a time insures that the sample vapor and N_2 dilution gas will become homogenously mixed prior to isotope analysis. After this mixing time, the sample bags are attached to an isotope ratio infrared spectrometer [see (8), Figure 3] (IWA-45EP off-axis integrated cavity output spectrometry, Los Gatos Research, San Jose, CA, USA). The IWA-45EP continuously monitors the isotope signature of incoming vapor when running in the water vapor isotope analyzer (WVIA) mode, or of discrete liquid samples when running in the liquid water isotope analyze (LWIA) mode. Running in the vapor mode, it continuously measures water vapor concentration, δ^2H, and $\delta^{18}O$ of incoming air. After the sampling bags were attached to the WVIA, measurement levels became stable after 2-3 minutes in agreement

with stabilization measurements presented by (Wassenaar et al. 2008). See Figure 7 below for an example time series of isotope and vapor concentration analysis.

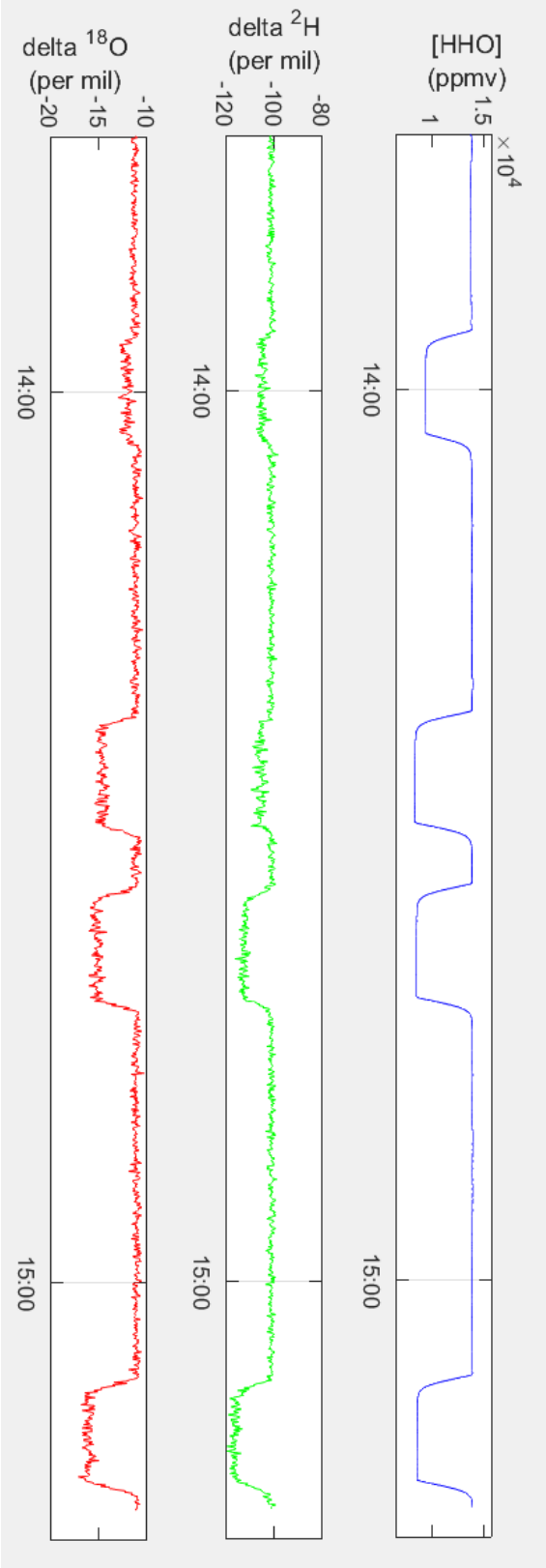

Figure 7 Typical isotope time series displaying water vapor concentrations and isotope ratios of three working standards and one unknown vapor sample. Note the similar water vapor mixing ratios of all 4 analyses.

The sample bags contained between 570-970 mL of volume for measurement, while the WVIA has an intake rate of between 70-100 mL per minute. Depending on the desired level of dilution, we were able to between 8 to 13 minutes of testing for each sample. Original efforts were in trying to come up with a closed-loop gas recirculation system so that smaller samples volumes could be tested for longer periods of time. Efforts within this regard were discontinued when a leaky internal pump on the WVIA was discovered that accounted a 0.5-1% per minute leak rate when running at low pressures (~40.22 torr) and at a sampling frequency of 0.2 Hz. Ambient room air was quickly entering the conveyance system when the system exhaust port was connected via FEP tubing to the sample inlet port, which in theory should have allowed for the continuous re-circling of sample. With the proposed method, we get around 6 to 11 minutes of analysis time after measurements stabilize, taking an average value of the last 3-5 minutes for the composite value of the vapor sample.

1.4.3 Principles Behind Procedures & Isotope Analysis

1.4.3.1 Standard Curve Correction, Humidity Correction

It is well established that IRIS instruments have a concentration dependent trend in measuring ^{18}O and ^{2}H (Aemisegger 2012). Many commercially available IRIS analytical instruments use gas nebulizers, or other liquid-water equilibrators to vaporize liquids of known isotopic composition. This provides a consistent reference over a period of time, and allows for better inter-lab comparisons of isotope results. In the case of our WVIA, we did not have access to a gas nebulizer, or water equilibrator to compare our raw machine measures of isotopes and vapor concentration to.

To remedy our inability to correct isotope and vapor concentration the traditional way, we ran three distinct waters in the LWIA mode at high replication against multiple manufacturer supplied liquid standards. The waters were all commercially available bottled waters. See the Table 3 below for a description of these waters.

Table 3 Working standards sourcing location, as well as treatment processes applied.

Standard	Location	Treatment	Source
FIJI Bottled Water	Yaqara, Viti Levu, Fiji Islands	None	Artesian Well
Lab D.I. Water	Atlanta, Georgia	Deionization	Chattahoochee River
Nice! Spring Water Bottled Water	Jackson County, Michigan	Micron Filtered, Ozonated, and UV	Spring

0.5 L of each of the three working standards were placed into insulated PTFE carboys approximately 20 L in volume [see (9), Figure 3]. Prior to the introduction of the liquid working standards, the carboys were flushed with N_2. The carboys are left to come into equilibrium, isotopically and thermodynamically. This happens on the order of a few minutes, as seen below in Figure 8.

175 mL of vapor is removed from the head space above the working standard within the carboys with the Hamilton 1-L Super Syringe, and then diluted using the same step as are done with diluting xylem water vapor [see (7), Figure 3]. The same volumetric sample to dilution gas ratio is used as the samples being tested. This acts as a correction factor in that now the differences in water vapor concentration do not need to be taken into account. All samples and standards were measured at the same relative water vapor concentration. Following the injection of the working standard and dilution gas, the same process for measuring and processing isotope values as was done with the samples was completed [see (5)-(8), Figure 3]. Analysis of working standards occurred during every sample analysis.

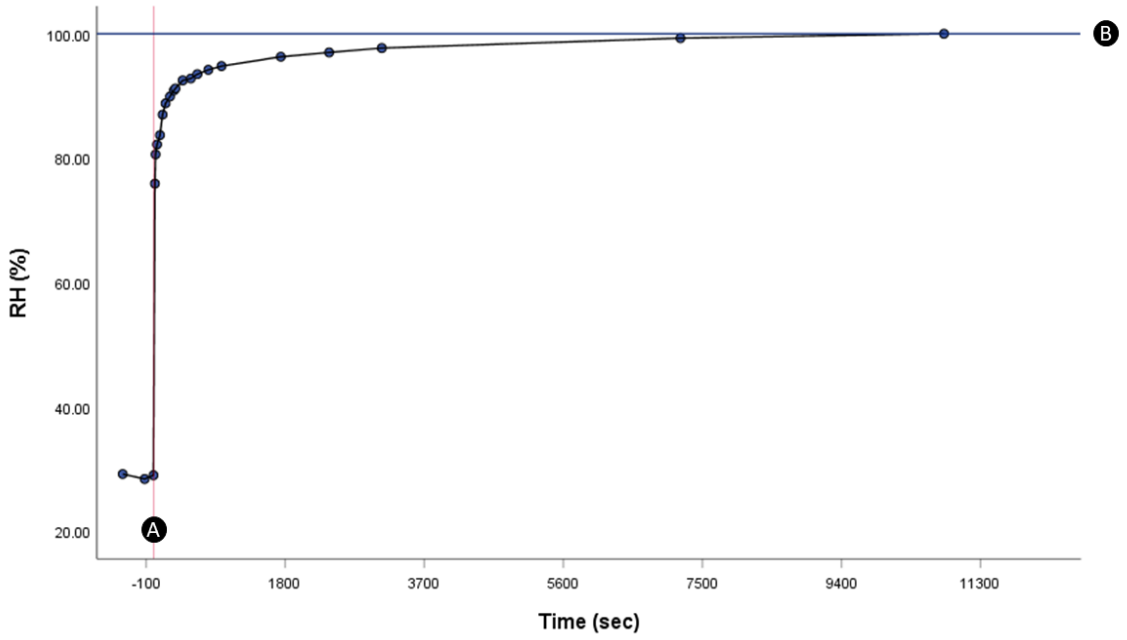

Figure 8 Working standard equilibration time series. Shows the amount of time it took to reach 100% RH in carboys storing working standards after the introduction of liquid water. (A) Introduction of liquid working standard (B) Point of 100% RH

1.4.3.2 Isotope Data Post-Processing

Following acquisition of mean isotope values for each of the three working standards, the raw vapor measurements were corrected based off the known liquid isotope composition measured using the LWIA. Subtracting the temperature-dependent fractionation factor, $10^3\ln(\alpha)$, from the known liquid isotope gives the projected isotope value for a vapor in isotopic and thermodynamic equilibrium with the source liquid. See Table 4 for a description of the coefficients used in applying Majoubes equation at different temperatures for $\delta^{18}O$ and $\delta^{2}H$ respectively. The coefficients and values for temperature-dependent fraction factors derived in Table 4 were taken from Clark and Fritz (1997), using the values published originally published by Majoube (1971), and further validated over a greater range of temperatures by Horita and Wesolowski (1994). The three raw measurements of working standards were plotted against their accompanying projected values. A simple linear regression was applied to determine a line of

Table 4 Temperature dependent fractionation factors. Factors for both ^{18}O and ^{2}H are shown at a range of temperatures. Based on the work of Majoube 1971

Water-Vapor Fractionation Factors		
T°C	**$10^3 \ln\alpha\,^{18}O_{w\text{-}v}$**	**$10^3 \ln\alpha_2\,^{2}H_{w\text{-}v}$**
-10	12.8	122
0	11.6	106
5	11.1	100
10	10.6	93
15	10.2	87
20	9.7	82
25	9.3	76
30	8.9	71
40	8.2	62
50	7.5	55
75	6.1	39
100	5.0	27

best fit to the three standards. The equation associated with that line of best fit was then applied to all raw measurement values of the working standards and samples, allowing for the raw machine measurements to standard-curve corrected. Coefficients of determination for standard curves ranged between 0.9037 and 1.0000. Standard curves, and their associated sample data were not used if the coefficient of determination was lower than 0.9000. Data were plotted on dual-isotope plots, along with the GMWL of Rozanski et al. (1993). Examining any deviation of measured values away from the GMWL provided one means of evaluating if any non-equilibrium, kinetic fractionation occurred during sampling and analysis. See Section 1.2.5 for a full description

1.5 Results

Table 5 below describes the equations and R^2 values for the working standard curve corrections done during each analysis. For δ^2H, the coefficient of determination ranged from 0.9693 to 0.9999, whereas for $\delta^{18}O$, these values ranged from 0.9037 to 0.9988. Mean values were 0.9909 and 0.9722 for δ^2H and $\delta^{18}O$ respectively. The slope derived from the δ^2H trendline ranged from 2.38 to 4.59 while the y-intercept ranged from a value of 161.90 to 372.46. For $\delta^{18}O$, slopes ranged from 1.03 to 3.02 and y-intercepts from 1.55 to 36.26.

Table 5 Coefficient of determination for each working standard analysis session. Additionally, the equations associated with each regression.

	^2H r^2	**^{18}O r^2**	**^2H eq**	**^{18}O eq**
11/6/2017	0.9987	0.9672	y =4.593x+372.46	y= 1.7427x+12.668
11/8/2017	0.9975	0.9976	y=3.3637x+256.23	y= 3.0175x+32.25
11/9/2017	1.0000	0.9901	y= 3.3117x+256.93	y=2.5947x+23.632
11/10/2017	0.9828	0.9942	y= 2.5481x+184.28	y= 2.1522x+26.947
11/14/2017	0.9693	0.9349	y= 2.7402x+196.46	y= 2.0372x+15.697
11/15/2017	0.9998	0.9629	y = 2.3751x+165.42	y= 1.2261x+8.3575
11/28/2017	0.9970	0.9942	y= 2.7043x+208.36	y= 1.0298x+1.5545
11/29/2017	0.9984	0.9988	y= 2.8239x+206.74	y= 1.5147x+7.7635
11/30/2017	0.9900	0.9793	y= 2.4913x+161.9	y= 1.8449x+11.889
12/1/2017	0.9833	0.9037	y= 3.6955x +290.73	y= 2.8374x+36.256
12/4/2017	0.9835	0.9716	y= 2.7795x+190.24	y = 1.6164x+ 10.268
Mean	**0.9909**	**0.9722**		

Average, curve-corrected values for each of the three working standards are displayed below in Table 6. Between our three standards, δ^2H had a range of ~42‰ and $\delta^{18}O$ had a range of ~5.5‰.

Table 6 Average composition of each of the working standards, included are mean residual errors and the dispersion of the measures at 1-standard deviation.

	^{2}H (‰)	^{18}O (‰)	^{2}H (‰) Error	^{18}O (‰) Error	1-σ ^{2}H (‰)	1-σ ^{18}O (‰)
Lab DI	-98.42	-13.4	0.74	0.23	0.69	0.31
FIJI	-123.12	-16.3	1.89	0.45	1.96	0.57
NICE Spring	-140.36	-18.68	1.15	0.22	1.28	0.28

Our most isotopically enriched standard, Lab DI, had a mean residual error of 0.74 ‰ for $\delta^{2}H$ and an error of 0.23 ‰ for $\delta^{18}O$ after correction. FIJI, the middle-value standard had an error of 1.89‰ for $\delta^{2}H$ and an error of 0.45 ‰ for $\delta^{18}O$ after correction. The most isotopically depleted standard, NICE Springs, had an error of 1.15 ‰ for $\delta^{2}H$ and an error of 0.22 ‰ for $\delta^{18}O$.

Table 7 Results from each time a species was tested, showing ^{2}H and ^{18}O error and the mean error from all the results. Included is the source water isotope values.

***Oxydendrum arboretum* (Sourwood)**				
Date	**^{2}H (‰)**	**^{18}O (‰)**	**^{2}H (‰) Error**	**^{18}O (‰) Error**
11/6/2017	-101.64	-16.40	2.96	3.10
11/8/2018	-95.54	-11.90	3.14	1.41
11/9/2017	-101.51	-17.16	2.84	3.85
11/10/2017	-101.03	-15.68	3.93	3.31
11/14/2017	-97.27	-13.15	1.41	0.16
11/15/2017	-87.21	-13.86	11.47	0.55
Average	**-97.37**	**-14.69**	**4.29**	**2.06**
***Fagus grandifolia* (American Beech)**				
Date	**^{2}H (‰)**	**^{18}O (‰)**	**^{2}H (‰) Error**	**^{18}O (‰) Error**
11/10/2017	-95.01	-14.55	1.91	1.89
11/14/2017	-91.87	-12.34	6.81	0.97
11/15/2017	-100.58	-14.15	1.91	0.85
12/1/2017	-98.07	-16.71	0.61	3.40
12/4/2017	-88.35	-13.84	10.32	0.53
Average	**-94.78**	**-14.32**	**4.31**	**1.53**
***Pinus taeda* (Loblolly Pine)**				
Date	**^{2}H (‰)**	**^{18}O (‰)**	**^{2}H (‰) Error**	**^{18}O (‰) Error**
11/29/2017	-106.42	-12.37	7.74	0.94
11/30/2017	-99.50	-10.30	0.83	3.01
12/4/2017	-89.68	-8.87	9.00	4.44
Average	**-98.53**	**-10.51**	**5.85**	**2.80**
Interspecies Mean	**-96.89**	**-13.17**	**4.82**	**2.13**
Source Water Composition	**-98.42**	**-13.40**	**0.73**	**0.23**

Table 7 reports the results from each sample of xylem water vapor that was analyzed. The isotopic signature was reported, along with the residual error associated with that measurement relative to the working standards. The known values of δ^2H and $\delta^{18}O$ for the source water the stems were transpiring were -98.42 ± 0.73‰ and -13.40 ± 0.23‰, respectively. Across all species, the arithmetic mean δ^2H was -96.89 ± 4.82‰ and the $\delta^{18}O$ -13.17 ± 2.13‰. Average values for *O. arboreum* were -97.37 ± 4.29‰ and -14.69 ± 2.06‰ for δ^2H and $\delta^{18}O$ respectively. Average values for *F. grandifolia* was -94.78 ± 4.31‰ and -14.32 ± 1.53‰ for δ^2H and $\delta^{18}O$ respectively. Average values for *P. taeda* was -98.53 ± 5.85‰ and -10.51 ± 2.80‰ for δ^2H and $\delta^{18}O$ respectively. These results are further displayed below in Figure 9.

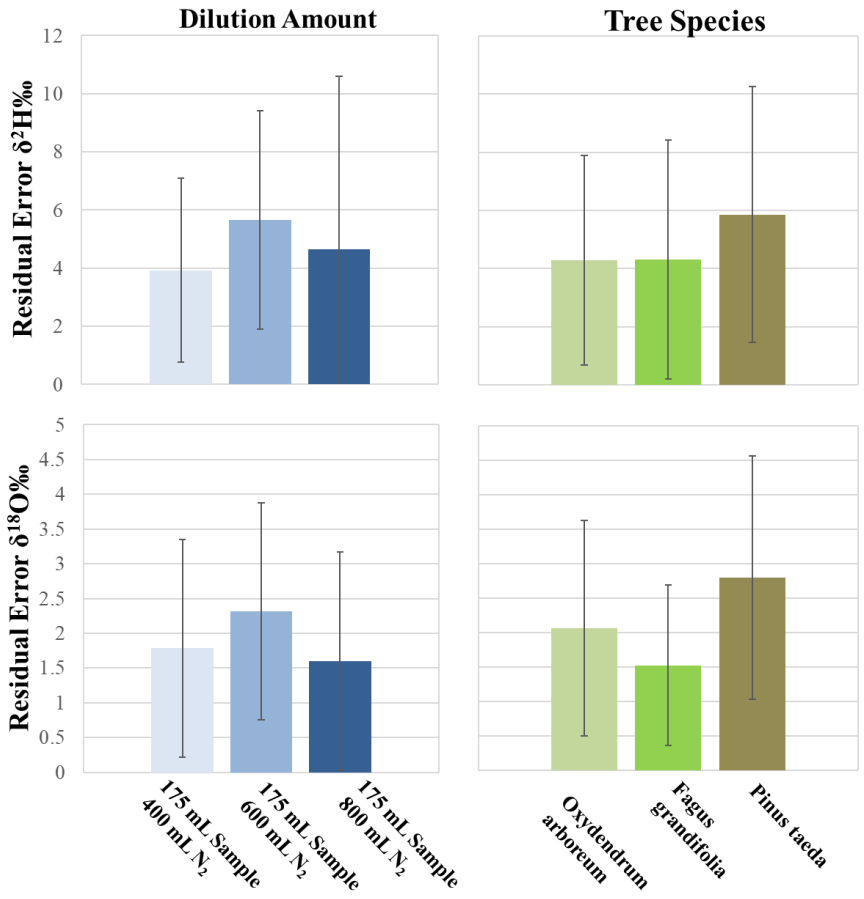

Figure 9 Tree type and effects of different humidity levels on residual errors. 400 mL of N_2 corresponds to an average mixing ratio of ~9,800 ppmv, 600 mL to ~8,700 ppmv, and 800 mL to ~8,000 ppmv. These ratios varied slightly from run to run.

The right side of the figure displays the residual errors of δ^2H and $\delta^{18}O$ measurements for each tree species, the left displays the residual errors across different N_2 dilution levels. Across all species, *P. taeda* displayed the greatest error in measurements both in δ^2H and $\delta^{18}O$ measurements, though there is a significant range of overlap among all species. Similarly, there was significant overlap for measurements across humidity levels.

Table 8 Average method error at the 3 water vapor mixing ratios (175 mL of sample with 400, 600, or 800 mL of N_2). Residual errors were greatest at the middle water vapor mixing ratio, 600 mL of N_2 (~8,700 ppmv).

175 mL to 400 mL					
Species	**Date**	**^2H (‰)**	**^{18}O (‰)**	**^2H (‰) Error**	**^{18}O (‰) Error**
Oxydendrum arboreum	11/9/2017	-101.51	-17.16	2.84	3.85
Oxydendrum arboreum	11/14/2017	-97.27	-13.15	1.41	0.16
Fagus grandifolia	11/14/2017	-91.87	-12.34	6.81	0.97
Pinus taeda	11/29/2017	-106.42	-12.37	7.74	0.94
Pinus taeda	11/30/2017	-99.50	-10.30	0.83	3.01
	Sample Average	**-99.31**	**-13.06**	**3.92**	**1.79**
175 mL to 600 mL					
Species	**Date**	**^2H (‰)**	**^{18}O (‰)**	**^2H (‰) Error**	**^{18}O (‰) Error**
Oxydendrum arboreum	11/8/2017	-95.54	-11.90	3.14	1.41
Oxydendrum arboreum	11/10/2017	-101.03	-15.68	3.93	3.31
Fagus grandifolia	11/10/2017	-95.01	-14.55	1.91	1.89
Fagus grandifolia	12/4/2017	-88.35	-13.84	10.32	0.53
Pinus taeda	12/4/2017	-89.68	-8.87	9.00	4.44
	Sample Average	**-93.92**	**-12.97**	**5.66**	**2.31**
175 mL to 800 mL					
Species	**Date**	**^2H (‰)**	**^{18}O (‰)**	**^2H (‰) Error**	**^{18}O (‰) Error**
Oxydendrum arboreum	11/6/2017	-101.64	-16.40	2.96	3.10
Oxydendrum arboreum	11/15/2017	-87.21	-13.86	11.47	0.55
Fagus grandifolia	11/15/2017	-100.58	-14.15	1.91	0.85
Fagus grandifolia	12/1/2017	-98.07	-16.71	0.61	3.40
	Sample Average	**-96.88**	**-15.28**	**4.24**	**1.97**

Table 8 displays the results of each sapling xylem water sample error across different water vapor mixing ratio ranges, from around 9,800 ppmv when 400 mL of N_2 is introduced, 8,700 ppmv for 600 mL of N_2, and 8,000 ppmv for 800 mL of N_2. Two runs at the same intended water vapor mixing ratio would vary on the order of 100-200 ppmv. Sample error for δ^2H ranged from

3.92‰ to 5.66‰, and the error for $\delta^{18}O$ ranged from 1.79‰ to 2.32‰. There does not seem to be an appreciable difference in error across humidity levels, the low (400 mL N_2) and high (800 mL N_2) dilutions have the lowest overall errors between δ^2H and $\delta^{18}O$, whereas the intermediate (600 mL N_2) dilution displayed the greatest error

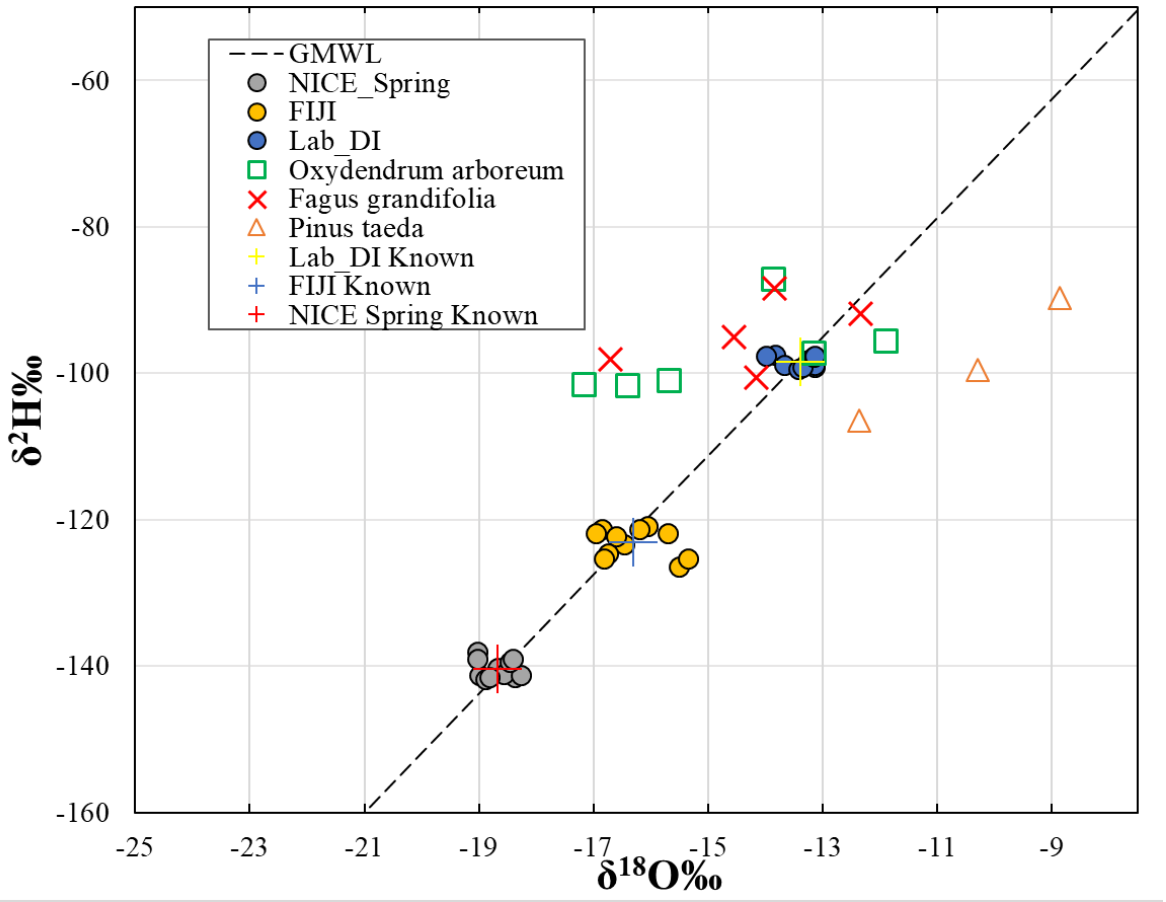

Figure 10 Dual isotope plot displaying data from all working standards and xylem vapor tests. The known isotope values of each working standard are marked, all xylem water samples have Lab_DI as their source water, and thus should plot as close as possible to that point. Points for working standards should be plotting as close to their known values as possible.

Figure 10 details the results of all the working standards and samples that were analyzed. These results are shown in a dual-isotope plot, comparing the δ^2H values to the $\delta^{18}O$ value of each measurement, all relative to the GMWL. Any deviation from the GMWL would indicate a

fractionating process that is impacting the vapor sample. For all of the samples, they should plot around Lab DI, as that was their source of water. The results for species *O. arboreum* and *F. grandifolia* are scattered around the working standard, with some significant deviations in $\delta^{18}O$ values for both. *P. taeda* results plot well off to the right of the GMWL in all cases. A full description of the values plotted in Figure 10 are displayed below in Tables 9 and 10.

Table 9 Full description of dual isotope plot results. Shows the date of analysis, dilution level, residual error, and mean isotope values for all working standards tested.

Nice Spring	**^{2}H (‰)**	**^{18}O (‰)**	**Dilution**	**^{2}H (‰) Error**	**^{18}O (‰) Error**
11/6/2017	-141.50	-18.37	165/800	0.46	0.40
11/8/2017	-140.30	-18.68	165/600	0.74	0.09
11/9/2017	-141.02	-18.57	165/400	0.02	0.20
11/10/2017	-141.22	-18.27	165/600	1.41	0.12
11/14/2017	-138.06	-19.02	165/400	2.98	0.26
11/15/2017	-141.23	-19.00	165/800	0.19	0.23
11/28/2017	-141.71	-18.88	165/400	0.68	0.12
11/29/2017	-141.54	-18.83	165/400	0.50	0.06
11/30/2017	-139.48	-18.47	165/400	1.56	0.30
12/1/2017	-138.96	-19.02	165/800	2.08	0.26
12/4/2017	-138.96	-18.40	165/600	2.07	0.36
FIJI	**^{2}H (‰)**	**^{18}O (‰)**	**Dilution**	**^{2}H (‰) Error**	**^{18}O (‰) Error**
11/6/2017	-121.30	-16.86	165/800	0.90	0.56
11/8/2017	-123.42	-16.46	165/600	1.22	0.15
11/9/2017	-122.25	-16.62	165/400	0.05	0.31
11/10/2017	-121.87	-16.97	165/600	3.20	0.24
11/14/2017	-126.36	-15.52	165/400	4.16	0.79
11/15/2017	-121.85	-15.70	165/800	0.35	0.60
11/28/2017	-120.85	-16.07	165/400	1.34	0.24
11/29/2017	-121.22	-16.20	165/400	0.97	0.11
11/30/2017	-124.60	-16.75	165/400	2.41	0.45
12/1/2017	-125.30	-15.36	165/800	3.11	0.95
12/4/2017	-125.29	-16.83	165/600	3.09	0.52
Lab_DI	**^{2}H (‰)**	**^{18}O (‰)**	**Dilution**	**^{2}H (‰) Error**	**^{18}O (‰) Error**
11/6/2017	-99.10	-13.15	165/800	0.42	0.16
11/8/2017	-98.18	-13.24	165/600	0.49	0.06
11/9/2017	-98.66	-13.19	165/400	0.01	0.11
11/10/2017	-98.83	-13.14	165/600	1.79	0.12
11/14/2017	-97.47	-13.84	165/400	1.21	0.53
11/15/2017	-98.84	-13.68	165/800	0.16	0.37
11/28/2017	-99.33	-13.43	165/400	0.66	0.12
11/29/2017	-99.14	-13.36	165/400	0.46	0.05
11/30/2017	-97.81	-13.16	165/400	0.87	0.14
12/1/2017	-97.65	-14.00	165/800	1.03	0.69
12/4/2017	-97.65	-13.15	165/600	1.03	0.16

Table 10 Full description of dual isotope plot results. Shows the date of analysis, dilution level, residual error, and mean isotope values for all the vapor samples tested.

Oxydendrum arboreum					
(Sourwood)	**^{2}H (‰)**	**^{18}O (‰)**	**Dilution**	**^{2}H (‰) Error**	**^{18}O (‰) Error**
11/6/2017	-101.64	-16.40	165/800	2.96	3.10
11/8/2017	-95.54	-11.90	165/600	3.14	1.41
11/9/2017	-101.51	-17.16	165/400	2.84	3.85
11/10/2017	-101.03	-15.68	165/600	3.93	3.31
11/14/2017	-97.27	-13.15	165/400	1.41	0.16
11/15/2017	-87.21	-13.86	165/800	11.47	0.55
Fagus grandifolia					
(Beech)	**^{2}H (‰)**	**^{18}O (‰)**	**Dilution**	**^{2}H (‰) Error**	**^{18}O (‰) Error**
11/10/2017	-95.01	-14.55	165/600	1.91	1.89
11/14/2017	-91.87	-12.34	165/400	6.81	0.97
11/15/2017	-100.58	-14.15	165/800	1.91	0.85
12/1/2017	-98.07	-16.71	165/800	0.61	3.40
12/4/2017	-88.35	-13.84	165/600	10.32	0.53
Pinus taeda					
(Pine)	**^{2}H (‰)**	**^{18}O (‰)**	**Dilution**	**^{2}H (‰) Error**	**^{18}O (‰) Error**
11/29/2017	-106.42	-12.37	165/400	7.74	0.94
11/30/2017	-99.50	-10.30	165/400	0.83	3.01
12/4/2017	-89.68	-8.87	165/600	9.00	4.44

1.6 Discussion

1.6.1 Deviations in the Working Standards

Variations in the isotopic composition of the liquid standards between runs could be the result of a number of processes. $\delta^{2}H$ and $\delta^{18}O$ values for the vapor of the working standards differed between runs, though were tightly dispersed, as seen in Tables 9-10. The values were constrained between 0.6883 to 1.9557‰ of one another for $\delta^{2}H$ and 0.2821 to 0.5731‰ $\delta^{18}O$ at one standard deviation. The standard that displayed the greatest residual error after each curve correction, FIJI, was also the working standard with the largest dispersion in measurement. It had the largest $\delta^{2}H$ and $\delta^{18}O$ deviation at 1.9557 and 0.5731‰ respectively. Investigating this on Figure 10, the dual isotope plot, shows the FIJI standard deviating from the GMWL in a pattern

indicating a type of kinetic fractionating process, or change in the overall isotopic composition of the liquid reservoir of the working standard.

The liquid working standards were analyzed in the liquid mode at the onset of the experimental period. Those $\delta^{2}H$ and $\delta^{18}O$ ratios were the values used throughout the course of the experiment as the composition of the water vapor in the liquid phase when employing the temperature-dependent fractionation factors to determine what the isotope composition of that same liquid should be in the vapor phase. All the liquid standards were stored in large volume PTFE carboys, which were presumably gas-tight to prevent any evaporation, or gas exchange with the surrounding environment. The liquid working standard could have been exposed to an extended period of vapor exchange with outside air which resulted in changes to the isotopic composition of the liquid source waters due to non-equilibrium physiochemical fractionation occurring. The resulting measured vapor would not have the correct liquid-state isotope value required to confidently apply the temperature dependent fractionation factors associated with the standard curve correction. This could easily be corroborated by remeasuring the liquid stored in these carboys to see if there has been a change in composition. Unfortunately, the liquid analysis capability of the laser spectrometer has been unavailable due to unforeseen technical problems since early December 2017.

Alternatively, this error could be explained by oversights and inattentiveness in vapor transfer, dilution, and transport prior to analysis. Given the systematic dispersion and residual error in standard measurement this seems less likely than the first explanation. The curve correction would be assuming that the environment which the vapor-liquid exchange is occurring in is complying with equilibrium fractionation conditions, meaning that any fractionating

processes would influence the liquid and vapor states in a similar fashion. This would mean that the subsequent vapor-state measurements would deviate from the GMWL.

1.6.2 Error in Water Vapor Concentrations

An explanation of some portion of the error in both standard measurement and vapor measurements could be the result of differences in water vapor concentration. Differences in water vapor concentrations were intended to be remedied by diluting all samples and standards with the same volume of N_2 calibration-quality gas. This dilution gas was introduced using a handheld syringe, expunged by hand. The apertures from the syringe, through the sample transfer lines, into the gas sampling bags were very small (<1/8”). While the connections are gas-tight when operated under ideal conditions, with manually introducing the gas, any sudden introduction would cause a major pressure rise, potentially compromising the integrity of the gas-impermeability of the fittings. If this occurred, we would have limited, if any, concept of the volume of dilution gas introduced to the sample. Without confidence that the standards and samples are having the same volume of dilution gas introduced, then the postulation that we do not need to correct for water vapor concentration cannot be assumed.

The WVIA gives the user a raw value of what the water vapor concentration is in parts per million volume. Without access to a gas nebulizer, or another analytical instrument which produces a vapor sample with a known water vapor concentration, we lacked the ability to corroborate the validity of these measurements relative to a standard. The machine was essentially running based on its factory calibration. Measurements of δ^2H are documented to be influenced by water vapor concentrations and water vapor mixing ratios. Sturm & Knohl (2010) found that the relationship between water vapor concentrations and analytical precision is non-linear, and uncorrected can account for a several per mil error (Sturm & Knohl 2010).

The residual errors associated with our sample and standard analysis follow the nonlinear trend as described by Sturm & Knohl (2010). Of the three water vapor concentrations we tested, the one with least amount of introduced dilution gas and subsequently the highest water vapor concentration, had the lowest residual error (Table 8). Consequently, the samples at the intermediate water vapor concentration had the highest residual error. The samples at the low water vapor concentration, which were expected to have the greatest error, as they had the least amount of water vapor relative to the dilution volume, had residual errors in-between that of the other high and middle water vapor concentrations. The relatively small (1-2‰) difference between each of these measures could again be accounted for due to unregimented sample transfer, or through the introduction of volatile organic compounds in the sample volume. These error levels are also within the range described by Sturm & Knohl (2010) as potential error due to uncorrected water vapor concentrations relative to a known concentration.

1.6.3 Interspecies Variations

Table 7 reports the results and mean values from each of species in the laboratory experiment. Mean δ^2H values for *O. arboreum* and *F. grandifolia* are quite similar, 4.29 and 4.31‰ respectively, but for the more resinous and sappy *P. taeda* the mean δ^2H value was 5.85‰. Isoprenes and terpenes more heavily concentrated and produced in the resinous *P. taeda* sapwood could easily be diffusing into our sampling apparatus. Once in the sample cavity, these VOC's would then be introduced into the analytical column of the WVIA during intake. VOC's are known to be a source of error in WS-CRDS, as they can have similar spectral absorbances as oxygen and hydrogen isotopes (Schultz et al. 2011). The reduced precision for *P. taeda* is further seen in δ^{18}O residual errors values. The more resinous *P. taeda* has the highest error for three tree species at 2.796‰. It is important to note that the test on *P. taeda* occurred at a later point in

time than the other species tested. This would have been during the period when we experienced poorer accuracy with measuring our working standards. While the decreased accuracy may have been due to the presence of organics, it could have also been because our instrument was operating at a different level of precision than during other test periods.

The precision of $\delta^{18}O$ and $\delta^{2}H$ measurements when running WS-CRDS instruments in liquid modes is generally on the order of ±1‰ for $\delta^{2}H$ and <0.2‰ for $\delta^{18}O$ (Volkmann and Weiler 2014). Similarly, with some of the other more sophisticated direct-vapor equilibration techniques described earlier, workers have achieved an accuracy similar to that of the liquid-based precision, ±0.34-0.39‰ for $\delta^{18}O$ and ±2.0-2.8‰ for $\delta^{2}H$, (Oerter et al. 2017; Volkmann and Weiler 2014). While the analytical precision is slightly lower for direct equilibration methods, the tradeoff is reduced sample preparation time and higher sample turnover.

1.6.4 Outlook of Diffusive Sampling Technique & Future Work

The diffusive technique we present for sampling xylem water had an analytical uncertainty of ±2.189‰ for $\delta^{18}O$ and ±4.819‰ for $\delta^{2}H$. This is significantly higher than comparative methods, especially in regard to $\delta^{18}O$. Regardless of the significant difference in analytical accuracy of our proposed method compared to traditional techniques, it still has application in ecohydrological studies that require less analytical accuracy, but better temporal resolution. Further, this method could potentially be adapted to other woody vegetation beyond just trees and saplings, in an effort to investigate similar water use questions as are interested in tree water uptake.

Large scale adoption of this technique will require workers to better understand and quantify the concentrations of volatile organic compounds being produced in the sapwood. The introduction of volatile organic compounds (VOC) into the intake of a wavelength-scanned

cavity ring down spectroscopy (WS-CRDS) is an established source of error. Testing of gas emanating from the sapwood through gas chromatography and mass spectrometry would give some insight into what chemical compounds are most present. Further, other spectral contaminants such as methane could be influencing isotopic measurements and need to be better considered. Diffusive transport of these gases along with the xylem water could be a portion of the residual errors we are seeing in our results, though that would be difficult to definitively say without further evidence. When running liquid water samples in the LWIA, there is proprietary software which detects and corrects for the introduction of these volatile compounds. When running water vapor samples in the WVIA, there is no such correction available.

Further along the path of spectral interference and measurement issues induced by the chemical properties of the xylem water vapor samples, is that of the differences in water vapor concentrations. Correcting for machine measurements with standards of known water vapor concentration and isotope composition will go a long way to constraining measurement errors.

Much of the presented technique is based on the premise that the vapor samples we are obtaining of xylem water are at 100% relative humidity. There were problems in obtaining that in a laboratory setting, our syringe-chamber design seemed to have some inherent barrier to diffusion in its design. Periodically extracted samples were measured with a psychrometer to check their humidity level, and most of the time they were not reaching thermodynamic equilibrium (i.e., 100% relative humidity). We further tested the gas impermeability of our sampling chambers by submerging one end into water, and measuring the time elapsed it would take for the syringes to come into equilibrium when close to a large, liquid reservoir. Again, we found that the volumes struggled to get to equilibrium conditions. To speed up diffusion and to test if our design was prone to leaking, we installed 5V micro-fans into the interior of acrylic

tubes submerged into water on one end. The fans were meant to disrupt the interior volume and speed up vapor mixing hoping the stagnant conditions within the sample volume were the source of the problem. Still, there seemed to be some barrier in our connections preventing diffusion, or a leak significant enough in both our sampling syringes and acrylic tube to compromise the gas impermeability of the design. The containers where standards are stored reached near-equilibrium on the order of minutes and maintained that condition for an extended period of time. A leak from both the syringe and the acrylic tube would explain the apparent inability to reach 100% relative humidity, as well as the deviations from the GMWL we saw in Figure 10. Alternatively, a yet unidentified barrier to vapor exchange between the Swagelok connections and sample volume could explain the same occurrence.

In assessing these results, it is important to take into account that these samples are taken as multiple water parcels travel up through the xylem. The diffused vapor we are testing is an integration of all of the water parcels that have traveled through the xylem area directly adjacent to the borehole in our chamber. While we are treating it as discrete samples taken at the time the syringe is detached, the vapor in the headspace has been in isotopic exchange with waters passing up through the xylem stream from the time the syringe with N_2 gas was attached. It also is an integrated measure of the waters traveling through the entire depth of the borehole. This could include water from the bark and cambium (unlikely as this is blocked by the Swagelok elbow) as well as the sapwood and heartwood. While the temporal integration would be difficult to get around, sampling ports could be installed at different heights on the trees, with the boreholes going to different depths. This would allow for sampling of the xylem water at different incremental depths along the flow paths.

1.7 Conclusion

Our proposed sampling method works off the direct liquid-vapor equilibration techniques that have developed in the past decade. We offer a fresh approach to sampling the stable isotope composition of xylem water, with a clear path forward on its needed improvements and limitations. If reliability, accuracy, and precision are improved upon, this would represent a significant step forward in the temporal ability to sample xylem water, while also reducing the sophistication and investment required. Improvements in these aspects would allow the implementation of this method in a field based experiment. Using deuterium-enriched waters as a tracer, we would be able to sample water vapor traveling through the transpiration stream at integrated time intervals. This ability, coupled with water extracted from different soil depths and storage reservoirs, along with water flux information in a watershed, would allow workers to better partition the relative contribution of transpiration in total evapotranspiration. Isotope mass balance equations utilize flux rates and mean isotope concentrations to provide providence to water parcels in a basin.

Applying this method in a tracer-based field application bring the benefit of seeing how the method stacks up when a high concentration of deuterated water is introduced to a system of isotopically depleted natural waters. Irrigating a section of the watershed with waters enriched δ^2H at a +100‰ concentration, whereas the natural waters are somewhere on the order of -140‰ to -10‰. Because ^{2}H is so limited in naturally occurring waters, the signal to noise ratio of the tracer to the background environment will still be very significant. A conservative estimate of that ratio would be at $\frac{+100 - -10‰\ \delta^2 H}{5‰\ \delta^2 H\ error}$, leaving a ratio of 22 to 1. We would be employing a method that has the ability to take samples more frequently than traditional methods but with a

potential measurement error of ~5‰. With that in mind, workers would need to consider if a 5‰ error would be acceptable given the application and desired outcomes of the method usage.

There are significant areas where improvements to the technique are needed. Ensuring that there are no barriers inhibiting vapor exchange between the liquid xylem water at the site of the port and the dry N_2 within sample volume is key. The premise behind the proposed technique requires thermodynamic, and isotopic equilibrium conditions be met in applying temperature dependent fractionation factors to infer the isotope composition of a liquid or its counterpart in the vapor phase. When these conditions are not in equilibrium, kinetic fractionating process come into play, moving the ratios of ^{2}H to ^{18}O away from the GMWL. Constraining leak points in connections, and in transfer to the analyzer would go a great deal towards limiting any of these fractionating processes from occurring.

The use of this method in ecohydrological studies measuring the stable isotopes of xylem water could provide an alternative to current methods. Cryogenic or azeotrophic distillation have been the traditional methods to extract water from xylem and soil, both of which require extensive sample preparation and have more recently it has been shown that cryogenic distillation (the foremost used method) has some problems. Alternatively, the development of sophisticated arrays of vapor permeable probes and continuous flow IRIS isotope analyzers give workers the option of fine temporal resolution for monitoring soil and xylem water isotope composition, with the tradeoff of a large initial time and fiscal investment. Further, these highly advanced and accurate arrays have limited field study applications without access to the mainline power required to power the isotope analyzers and their subsequent pumps. Field studies using the distillation techniques typically are able to sample trees on the order of 1-2 times a day at the beginning of a study period, and then at the minimum of a weekly scale thereafter. This is given

in part due to the time constraints in sample preparation, but also due to the limitation in destructively sampling xylem tissue on the same tree a repeated number of times.

Taking into account the limitations and inherent errors in our diffusive sampling procedure, it has value in the tracer based field experiments described previously. The benefit provided by that type of ecohydrological experiment is in its ability to provide an on the ground, field based estimate of the proportion transpiration contributes to evapotranspiration in an experimental catchment. These physical based estimates of T/ET from small experimental watersheds whose physical properties (forest type, land use, soil characteristics, groundwater behavior, etc) have been extensively inventories, are valuable as they can be used to validate and scale up climate models to better estimate the global mean contribution of transpiration in evapotranspiration.

REFERENCES

Aemisegger, F., et al. (2012) Measuring variations of [delta] 18O and [delta] 2H in atmospheric water vapour using two commercial laser-based spectrometers: an instrument characterisation study. Atmospheric Measurement Techniques 5(7): 1491.

Allen, R. G., L. S. Pereira, D. Raes & M. Smith (1998) Crop evapotranspiration-Guidelines for computing crop water requirements-FAO Irrigation and drainage paper 56. FAO, Rome, 300, D05109.

Beyer, M., et al. (2016). A deuterium-based labeling technique for the investigation of rooting depths, water uptake dynamics and unsaturated zone water transport in semiarid environments. Journal of Hydrology 533(Supplement C): 627-643.

Brooks, J. R., H. R. Barnard, R. Coulombe & J. J. McDonnell (2009) Ecohydrologic separation of water between trees and streams in a Mediterranean climate. Nature Geoscience, 3, 100.

Brunel, J. P., G. R. Walker, J. C. Dighton & B. Monteny (1997) Use of stable isotopes of water to determine the origin of water used by the vegetation and to partition evapotranspiration. A case study from HAPEX-Sahel. Journal of Hydrology, 188, 466-481.

Čermák, J., J. Kučera, W. L. Bauerle, N. Phillips & T. M. Hinckley (2007) Tree water storage and its diurnal dynamics related to sap flow and changes in stem volume in old-growth Douglas-fir trees. Tree physiology, 27, 181-198.

Chang, Elliot, et al. (2016) Improved removal of volatile organic compounds for laser-based spectroscopy of water isotopes. Rapid Communications in Mass Spectrometry 30.6: 784-790.

Coenders-Gerrits, A., R. Van der Ent, T. Bogaard, L. Wang-Erlandsson, M. Hrachowitz & H. Savenije (2014) Uncertainties in transpiration estimates. Nature, 506, E1.

Clark, I. D. & P. Fritz. 1997. Environmental isotopes in hydrogeology. CRC press.

Dansgaard, W. (1964) Stable isotopes in precipitation. Tellus, 16, 436-468.

Dawson, T. E. (1993). Hydraulic lift and water use by plants: implications for water balance, performance and plant-plant interactions. Oecologia 95(4): 565-574.

Dawson, T. E. (1998). Fog in the California redwood forest: ecosystem inputs and use by plants. Oecologia 117(4): 476-485.

De Graaf, R. & J. Van den Ende (1981) Transpiration and evapotranspiration of the glasshouse crops. In III International Symposium on Water supply and Irrigation in the open and under Protected Cultivation 119, 147-158.

Ehleringer, J. R., & Dawson, T. E. (1992) Water uptake by plants: perspectives from stable isotope composition. Plant, Cell & Environment, 15(9), 1073-1082.

Ehleringer, J. R., J. Roden & T. E. Dawson (2000) Assessing Ecosystem-Level Water Relations Through Stable Isotope Ratio Analyses. In Methods in Ecosystem Science, eds. O. E. Sala, R. B. Jackson, H. A. Mooney & R. W. Howarth, 181-198. New York, NY: Springer New York.

Evaristo, J., et al. (2015). Global separation of plant transpiration from groundwater and streamflow. Nature 525(7567): 91.

Fetter, C. W. (2000) Applied Hydrogeology. Prentice Hall.

Fritschen, L. J. & R. Shaw (1961) Transpiration and Evapotranspiration of Corn as Related to Meteorological Factors 1. Agronomy Journal, 53, 71-74.

Gaines, K. P., et al. (2016). Rapid tree water transport and residence times in a Pennsylvania catchment. Ecohydrology 9(8): 1554-1565.

Gaines, K. P., J. W. Stanley, F. C. Meinzer, K. A. McCulloh, D. R. Woodruff, W. Chen, T. S. Adams, H. Lin & D. M. Eissenstat (2016) Reliance on shallow soil water in a mixed-hardwood forest in central Pennsylvania. Tree Physiology, 36, 444-458.

Gaj, M., M. Beyer, P. Koeniger, H. Wanke, J. Hamutoko & T. Himmelsbach (2016) In situ unsaturated zone water stable isotope (2 H and 18 O) measurements in semi-arid environments: a soil water balance. Hydrology and Earth System Sciences, 20, 715.

Good, S. P., D. Noone & G. Bowen (2015) Hydrologic connectivity constrains partitioning of global terrestrial water fluxes. Science, 349, 175-177.

Gupta, P., D. Noone, J. Galewsky, C. Sweeney & B. H. Vaughn (2009) Demonstration of high-precision continuous measurements of water vapor isotopologues in laboratory and remote field deployments using wavelength-scanned cavity ring-down spectroscopy (WS-CRDS) technology. Rapid Communications in Mass Spectrometry, 23, 2534-2542.

Horita, J. & D. J. Wesolowski (1994) Liquid-vapor fractionation of oxygen and hydrogen isotopes of water from the freezing to the critical temperature. Geochimica et Cosmochimica Acta, 58, 3425-3437.

Hsieh, J. C., O. A. Chadwick, E. F. Kelly & S. M. Savin (1998) Oxygen isotopic composition of soil water: quantifying evaporation and transpiration. Geoderma, 82, 269-293.

Jasechko, S., Z. D. Sharp, J. J. Gibson, S. J. Birks, Y. Yi & P. J. Fawcett (2013) Terrestrial water fluxes dominated by transpiration. Nature, 496, 347-350.

Kalma, S. J., et al. (1998). A comparison of heat pulse and deuterium tracing techniques for estimating sap flow in Eucalyptus grandis trees. Tree physiology 18(10): 697-705.

Koehler, G. & L. I. Wassenaar (2011) Realtime Stable Isotope Monitoring of Natural Waters by Parallel-Flow Laser Spectroscopy. Analytical Chemistry, 83, 913-919.

Koehler, G., L. I. Wassenaar & M. J. Hendry (1999) An automated technique for measuring δD and δ18O values of porewater by direct CO2 and H2 equilibration. Analytical chemistry, 72, 5659-5664.

Koeniger, P., C. Leibundgut, T. Link & J. D. Marshall (2010) Stable isotopes applied as water tracers in column and field studies. Organic Geochemistry, 41, 31-40.

Kurita, N., et al. (2012) Evaluation of continuous water vapor [delta] D and [delta] 18O measurements by off-axis integrated cavity output spectroscopy. Atmospheric Measurement Techniques 5.8: 2069.

Lambs, L. & A. Saenger (2011) Sap flow measurements of Ceriops tagal and Rhizophora mucronata mangrove trees by deuterium tracing and lysimetry. Rapid Communications in Mass Spectrometry, 25, 2741-2748.

Liu, C., X. Zhang & Y. Zhang (2002) Determination of daily evaporation and evapotranspiration of winter wheat and maize by large-scale weighing lysimeter and micro-lysimeter. Agricultural and Forest Meteorology, 111, 109-120.

Majoube, M. (1971) Fractionnement en oxygene 18 et en deuterium entre l'eau et sa vapeur. Journal de Chimie Physique, 68, 1423-1436.

Marc, V. and M. Robinson (2004). Application of the deuterium tracing method for the estimation of tree sap flow and stand transpiration of a beech forest (Fagus silvatica L.) in a mountainous Mediterranean region. Journal of Hydrology 285(1–4): 248-259.

Maxwell, R. M. & L. E. Condon (2016) Connections between groundwater flow and transpiration partitioning. Science, 353, 377-380.

McCarroll, D. & N. J. Loader (2004) Stable isotopes in tree rings. Quaternary Science Reviews, 23, 771-801.

McCutcheon, R. J., J. P. McNamara, M. J. Kohn & S. L. Evans (2017) An evaluation of the ecohydrological separation hypothesis in a semiarid catchment. Hydrological Processes, 31, 783-799.

Meinzer, F. C., et al. (2006). "Dynamics of water transport and storage in conifers studied with deuterium and heat tracing techniques." Plant, Cell & Environment 29(1): 105-114.

Munksgaard, N. C., C. M. Wurster & M. I. Bird (2011) Continuous analysis of delta O-18 and delta D values of water by diffusion sampling cavity ring-down spectrometry: a novel sampling device for unattended field monitoring of precipitation, ground and surface waters. Rapid Communications in Mass Spectrometry, 25, 3706-3712.

Munksgaard NC, Cheesman AW, Wurster CM, Cernusak LA, Bird MI. (2014) Microwave extraction–isotope ratio infrared spectroscopy (MEIRIS): a novel technique for rapid extraction and in-line analysis of δ 18O and δ 2 H values of water in plants, soils and insects. Rapid Communications in Mass Spectrometry 28(20): 2151–2161. DOI:10.1002/rcm.7005.

Oerter, E. J., A. Perelet, E. Pardyjak & G. Bowen (2017) Membrane inlet laser spectroscopy to measure H and O stable isotope compositions of soil and sediment pore water with high sample throughput. Rapid Communications in Mass Spectrometry, 31, 75-84.

Orlowski, N., L. Breuer & J. J. McDonnell (2016a) Critical issues with cryogenic extraction of soil water for stable isotope analysis. Ecohydrology, 9, 1-5.

Orlowski, N., H.-G. Frede, N. Brüggemann & L. Breuer (2013) Validation and application of a cryogenic vacuum extraction system for soil and plant water extraction for isotope analysis. Journal of Sensors and Sensor Systems, 2, 179-193.

Orlowski, N., D. L. Pratt & J. J. McDonnell (2016b) Intercomparison of soil pore water extraction methods for stable isotope analysis. Hydrological Processes, n/a-n/a.

Parker, L. V. & T. A. Ranney (1994) Effect of concentration on sorption of dissolved organics by PVC, PTFE, and stainless steel well casings. Groundwater Monitoring & Remediation, 14, 139-149.

Piayda, A., et al. (2017). Quantification of dynamic soil–vegetation feedbacks following an isotopically labelled precipitation pulse. Biogeosciences 14(9): 2293.

Peterson, B. J. & B. Fry (1987) Stable isotopes in ecosystem studies. Annual review of ecology and systematics, 18, 293-320.

Roffael, E. (2006) Volatile organic compounds and formaldehyde in nature, wood and wood based panels. Holz als Roh-und Werkstoff, 64, 144-149.

Rothfuss, Y., S. Merz, J. Vanderborght, N. Hermes, A. Weuthen, A. Pohlmeier, H. Vereecken & N. Brüggemann (2015) Long-term and high-frequency non-destructive monitoring of

water stable isotope profiles in an evaporating soil column. Hydrol. Earth Syst. Sci., 19, 4067-4080.

Rozanski, K., et al. (1993) Isotopic patterns in modern global precipitation. Climate change in continental isotopic records: 1-36.

Rübel, A. P., C. Sonntag, J. Lippmann, F. Pearson & A. Gautschi (2002) Solute transport in formations of very low permeability: Profiles of stable isotope and dissolved noble gas contents of pore water in the Opalinus Clay, Mont Terri, Switzerland. Geochimica et Cosmochimica Acta, 66, 1311-1321.

Schwendenmann, L., et al. (2010). Can deuterium tracing be used for reliably estimating water use of tropical trees and bamboo? Tree physiology 30(7): 886-900.

Schwinning, S., et al. (2002). Deuterium enriched irrigation indicates different forms of rain use in shrub/grass species of the Colorado Plateau. Oecologia 130(3): 345-355.

Schlesinger, W. H. & S. Jasechko (2014) Transpiration in the global water cycle. Agricultural and Forest Meteorology, 189, 115-117.

Schultz, N. M., Griffis, T. J., Lee, X., and Baker, J.M. (2011) Identification and correction of spectral contamination in 2H/1H and 18O/16O measured in leaf, stem, and soil water, Rapid Commun. Mass Spectrom., 25, 3360–3368, doi:10.1002/rcm.5236,

Sturm, P. and A. Knohl (2010). Water vapor delta 2H and delta 18 O measurements using off-axis integrated cavity output spectroscopy. Atmos. Meas. Tech. 3(1): 67-77.

Teskey, R. O., T. M. Hinckley & C. C. Grier (1983) Effect of interruption of flow path on stomatal conductance of Abies amabilis. Journal of Experimental Botany, 34, 1251-1259

Volkmann, T. H. M., K. Kühnhammer, B. Herbstritt, A. Gessler & M. Weiler (2016) A method for in situ monitoring of the isotope composition of tree xylem water using laser spectroscopy. Plant, Cell & Environment, 39, 2055-2063.

Volkmann, T. H. M. & M. Weiler (2014) Continual in situ monitoring of pore water stable isotopes in the subsurface. Hydrol. Earth Syst. Sci., 18, 1819-1833.

Wassenaar, L. I. and G. Koehler (1999). An on-line technique for the determination of the δ18O and δ17O of gaseous and dissolved oxygen. Analytical Chemistry 71(21): 4965-4968.

Wassenaar, L. I., M. J. Hendry, V. L. Chostner & G. P. Lis (2008) High Resolution Pore Water δ2H and δ18O Measurements by H2O(liquid)−H2O(vapor) Equilibration Laser Spectroscopy. Environmental Science & Technology, 42, 9262-9267.

Williams, D. G., et al. (2004). Evapotranspiration components determined by stable isotope, sap flow and eddy covariance techniques. Agricultural and Forest Meteorology 125(3–4): 241-258.

White, J. W., Cook, E. R., & Lawrence, J. R. (1985). The DH ratios of sap in trees: Implications for water sources and tree ring DH ratios. Geochimica et Cosmochimica Acta, 49(1), 237-246.

Yepez, E. A., et al. (2005). Dynamics of transpiration and evaporation following a moisture pulse in semiarid grassland: A chamber-based isotope method for partitioning flux components. Agricultural and Forest Meteorology 132(3–4): 359-376.

Zhao, L., et al. (2011). Detailed assessment of isotope ratio infrared spectroscopy and isotope ratio mass spectrometry for the stable isotope analysis of plant and soil waters. Rapid Communications in Mass Spectrometry 25(20): 3071-3082.